

**ISLAMIC UNIVERSITY OF TECHNOLOGY  
(IUT)**

**IMPROVEMENT IN DISCONTINUOUS RECEPTION (DRX) POWER  
SAVING FOR NONREAL-TIME TRAFFIC IN  
LONG TERM EVOLUTION (LTE)**

BY

MD. ATIQUL ISLAM  
MD. MEHADI HASSAN  
ZOBAYER AHMED  
RAFID HASAN

A Dissertation

Submitted in Partial Fulfillment of the Requirement for the  
**Bachelor of Science in Electrical and Electronic Engineering**  
Academic Year: 2014-2015

Department of Electrical and Electronic Engineering.  
Islamic University of Technology (IUT)  
A Subsidiary Organ of OIC  
Dhaka, Bangladesh.

A Dissertation on

**Improvement in Discontinuous Reception (DRX)  
Power Saving for Nonreal-Time Traffic in  
Long Term Evolution (LTE)**

Submitted by

---

MD. ATIQUL ISLAM

---

MD. MEHADI HASSAN

---

ZOBAYER AHMED

---

RAFID HASAN

Approved By

---

PROF. DR. MD. SHAHID ULLAH

Head of the Department

Department of Electrical and Electronic Engineering

Islamic University of Technology (IUT)

Gazipur-1704, Bangladesh.

Supervised by

---

Mohammad Tawhid Kawser

Assistant Professor

Department of Electrical and Electronic Engineering

Islamic University of Technology (IUT)

---

## **ACKNOWLEDGEMENTS**

---

We express our heartiest gratefulness to Almighty Allah for His divine blessings, which made us able to complete this thesis successfully.

The thesis was carried out by the authors under the close supervision of Mohammad Tawhid kawser, Assistant Professor, Department of Electrical and Electronic Engineering, Islamic University of Technology (IUT). He had dedicated his valuable time to ensure the completion of this thesis. We express profound gratitude to him for his support, cooperation and guidance in accomplishing the thesis.

We wish to take this opportunity to express our sincerest gratitude and heartiest thanks to our parents and family members for being such delightful people and the inspiration for our effort. Without their prayers, continued encouragement, moral and financial support, it would not have been easy for us to accomplish this work, indeed their reward is with the Almighty Allah.

We also would like to thank our friends, colleagues and whoever helped us in the course of our work and or write-up.

Excuse us for any errors that might occur in this report despite of our best efforts.

---

## Abstract

---

The discontinuous reception (DRX) operation is included in long term evolution (LTE) to achieve power saving and prolonged battery life of the UE. An improvement in DRX power saving usually leads to a potential increase in the packet delay. An optimum DRX configuration depends on the current data traffic, which is not easy to estimate accurately, especially, for nonreal-time applications.

In our thesis, we propose a novel way to vary the DRX cycle length avoiding continuous estimation of the data traffic when only nonreal-time applications are running with no real-time applications active. Since small delay in nonreal-time traffic does not essentially impact the user's experience adversely, we allow limited amount of delay deliberately in our proposal to attain significant improvement in power saving. Our proposal also improves the delay in service resumption after a long inactivity. We use a stochastic analysis assuming M/G/1 queue to validate the improvement of the proposal.

**Keywords:** LTE, DRX, nonreal-time traffic, power saving.

---

# Contents

---

<b>Abstract</b>	<b>iv</b>
<b>Contents</b>	<b>v</b>
<b>List of Tables</b>	<b>vii</b>
<b>List of Figures</b>	<b>viii</b>
<b>Abbreviations</b>	<b>ix</b>
<b>1 Introduction</b>	<b>1</b>
1.1 Thesis Objectives .....	3
1.2 Study Methodology .....	3
1.2.1 The Simulator .....	4
1.3 Thesis Outlines .....	4
<b>2 Long Term Evolution (LTE)</b>	<b>5</b>
2.1 LTE System Attributes .....	6
2.2 LTE Network Structure .....	7
2.2.1 Layer 2 Structure .....	10
2.2.2 Radio Resource Control (RRC) States .....	12
<b>3 Existing DRX Mechanism</b>	<b>13</b>
3.1 DRX in RRC_IDLE State .....	13
3.2 DRX in RRC_CONNECTED State .....	14
3.2.1 Configuration of the DRX Cycle .....	15
3.2.2 Continuous Reception and Resumption of DRX .....	16
3.2.3 HARQ During DRX .....	17
3.2.4 Active Time .....	19
3.3 Depictment of All DRX States .....	19

<b>4 Proposed DRX Scheme</b>	<b>21</b>
<b>5 Analytical Model</b>	<b>24</b>
5.1 Different Power Saving Factors .....	24
5.2 Proposed Power Saving Factor .....	25
5.3 Mean Duration of DRX Operation .....	26
5.4 Mean Duration of Running Inactivity Timer .....	29
5.5 Mean Duration of Data Transfer .....	30
5.6 Delay Performance .....	32
<b>6 Simulation Results</b>	<b>35</b>
6.1 Simulation Assumptions .....	35
6.2 Simulation Output .....	36
<b>7 Conclusion</b>	<b>42</b>
7.1 Future Works .....	43
<b>Bibliography</b>	<b>44</b>

---

## List of Tables

---

Table 1.1	Characteristics of RT and NRT Traffic . . . . .	2
Table 2.1	LTE System Attributes . . . . .	6
Table 6.1	Simulation Assumptions . . . . .	36

---

## List of Figures

---

Figure 2.1 LTE Network Structure .....	7
Figure 2.2 Functional split between eNB and MME/GW .....	8
Figure 2.3 User Plane Protocol .....	9
Figure 2.4 Control Plane Protocol Stack .....	9
Figure 2.5 Downlink Layer 2 Structure .....	11
Figure 2.6 Uplink Layer 2 Structure .....	11
Figure 3.1 On Duration and DRX period in DRX Cycle.....	14
Figure 3.2 Total DRX Cycles with short and long cycles .....	15
Figure 3.3 PDU Loss Detection with HARQ Recording .....	16
Figure 3.4 States associated with DRX .....	19
Figure 4.1 Proposed DRX Mechanism .....	22
Figure 6.1 Percentage power consumption vs. packet arrival (case 1) .....	36
Figure 6.2 Relative DRX period vs. packet arrival rate (case 1) .....	37
Figure 6.3 Overall packet delay vs. packet arrival rate (case 1) .....	38
Figure 6.4 Percentage power consumption vs. packet arrival (case 2) .....	38
Figure 6.5 Overall packet delay vs. packet arrival rate (case 2) .....	39
Figure 6.6 Delay in service resumption vs. packet arrival rate (case 1 and case 2) ...	40
Figure 6.7 Percentage power consumption vs. packet arrival (case 3) .....	40
Figure 6.8 Overall packet delay vs. packet arrival rate (case 2) .....	41



---

## Abbreviations

---

3G	Third Generation
3GPP	3rd Generation Partnership Project
ACK	Acknowledgement
AM	Acknowledged Mode
AMR	Adaptive Multirate
AVI	Actual Value Interface
ARQ	Automatic Repeat Request
BLER	Block Error Rate
BSR	Buffer Status Report
CC	Chase Combining
CP	Cycling Prefix
CQI	Channel Quality Indicator
CS	Circuit Switched
DFT	Discrete Fourier Transform
DFT-SOFDM	DFT Spread OFDM
DRX	Discontinuous Reception
EDGE	Enhanced Data rates for GSM Evolution
EESM	Exponential Effective SINR Metric

EUTRAN	Evolved Universal Terrestrial Radio Access Network
eNodeB	Evolved Node B
EPS	Evolved Packet System
FDD	Frequency Division Duplexing
FDMA	Frequency Division Multiple Access
FTP	File Transfer Protocol
GBR	Guarantee Bit Rate
GERAN	GSM EDGE Radio Access Network
GSM	Global System for Mobile Communications
GW	Gateway
HARQ	Hybrid Automatic Repeat Request
HSPA	High Speed Data Access
ICIC	Inter-Cell Interference Coordination
IMT-2000	International Mobile Telecommunications-2000
IP	Internet Protocol
IR	Incremental Redundancy
ISI	Inter-symbol Interference
LTE	Long Term Evolution
MAC	Medium Access
MCS	Modulation and Coding Scheme
MIMO	Multiple Input Multiple Output
MISO	Multiple Input Single Output
MME	Mobility Management Entity
MRC	Maximum Ratio Combining
NAS	Non-Access Stratum
NACK	Non-Acknowledgement

NRT	Nonreal-Time
OFDM	Orthogonal Frequency Division Multiplexing
OFDMA	Orthogonal Frequency Division Multiple Access
PAPR	Peak-To-Average Power Ratio
PCEF	Policy and Charging Enforcement Function
PDA	Personal Digital Assistant
PDB	Packet delay budget
PDCCH	Physical Downlink Control Channel
PDCP	Packet Data Convergence Protocol
PDSCH	Physical Downlink Shared Channel
PDN	Packet Data Network
PDU	Packet Data Units
PELR	Packet error loss rate
PO	Paging Occasion
PRB	Physical Resource Block
PUCCH	Physical Uplink Control Channel
PUSCH	Physical Uplink Shared Channel
P-GW	PDN Gateway
QAM	Quadrature Amplitude Modulation
QoS	Quality of Service
QPSK	Quadrature Phase Shift Keying
RAN	Radio Access Network
RAT	Radio Access Technology
RB	Resource Block
RF	Radio Frequency
RLC	Radio Link Control

RNC	Radio Network Control
RR	Resource Request
RRC	Radio Resource Control
RRM	Radio Resource Management
RT	Real-Time
RTT	Round Trip Time
SAE	System Architecture Evolution
SAW	Stop and wait
SC	Single Carrier
SC-FDMA	Single Carrier Frequency Division Multiple Access
SID	Silence Descriptor
SIMO	Single Input Multiple
SINR	Signal to Interference-Plus-Noise Ratio
SR	Scheduling Request
SRS	Sounding Reference Signal
S-GW	Serving Gateway
TDD	Time Division Duplexing
TSG	Technical Specifications Group
TTI	Transmission Time Interval
UE	User Equipment
UM	Unacknowledged Mode
UTRAN	Universal Terrestrial Radio Access Network
VAD	Voice Activity Detector
VoIP	Voice over Internet Protocol
WCDMA	Wideband Code Division Multiple Access
WLAN	Wireless Local Area Network

# Chapter 1

---

## Introduction

---

The availability of more and more powerful hardware in mobile computation systems makes these devices the future platform for the development of a large set of new applications that will open new business models and will increase the market penetration in current society. However, the multitude and complexity of components needed to implement a large number of communications protocols makes the evaluation of power efficiency one of the tightest issues. In fact, the performance and utility of distributed systems is impacted by the availability of participating nodes. Each one of these must be connected to another to ensure remote task execution and data consistency, in an always on manner. This particular objective, hard to be achieved in wired network, is even more tricky in mobile environments. Mobile devices show the unwelcome peculiarity of a finite lifetime [29]. The power consumption of PDAs and smartphones represents a very complex problem, because of the number of physical components of the system, each with its own consumption value (backlight, Bluetooth module, Wireless Local Area Network (WLAN) module, phone module, other circuits, etc.).

The important fact is that the energy demands of battery powered devices, added to the software applications behaviors substantially exceed the capacity of the actual battery technology. The development of new architectures and procedures to build power-efficient and power-aware systems has become one of the main purposes in the design of new mobile communication systems. New generation mobile communication systems like Long Term Evolution (LTE) aim to deploy to customers a new mobile experience providing higher data rates and lower latencies that can make wireless devices a great

platform to run a new whole set of services and applications, which was unimaginable just some years ago.

This causes the battery of the user equipment (UE) to drain out quickly and the battery power saving has become a significant concern. The key technique to save power and prolong battery life is to let the UE switch off the receiver circuitry periodically. This is referred to as discontinuous reception (DRX). The periodic cycle in DRX, consisting of an active and an inactive period, is called DRX cycle [1]. The DRX parameters, especially, the DRX cycle length, involves a trade-off between power saving and packet delay.

The data traffic can be classified as following two types:

- Real-time (RT)
- Nonreal-time (NRT).

The RT applications include voice, live streaming video, online gaming, etc.

The NRT applications include buffered streaming video, web browsing, e-mail, chat, FTP, P2P file sharing, etc. The quality-of-service (QoS) requirements are quite different between RT and NRT traffic. RT traffic has a stringent delay requirement, while some level of packet loss rate can be acceptable. Conversely, NRT traffic is error-sensitive but the transmission delay can be larger. For each of the EPS bearers in LTE, a packet delay budget (PDB) is defined, which indicates an upper limit for packet delay between the UE and the policy and charging enforcement function (PCEF) in the core network. The delay should not exceed PDB in the case of 98% of the packets that have not been dropped due to congestion. Similarly, a packet error loss rate (PELR) is defined for each of the EPS bearers. The PELR is typically,  $10^{-3}$  and  $10^{-6}$  for RT and NRT traffic, respectively. The PDB is typically, 100 ms and 300 ms for RT and NRT traffic, respectively [7].

Characteristics	Real-time (RT) Traffic	Nonreal-time (NRT) Traffic
Packet error loss rate (PELR)	$10^{-3}$	$10^{-6}$
Packet delay budget (PDB)	100 ms	300 ms

**Table 1.1** Characteristics of RT and NRT Traffic

Thus, the NRT traffic permits the delay requirement to slacken to some extent. In other words, a limited amount of delay can be allowed to NRT traffic essentially with no adverse impact on the user's experience.

## 1.1 Thesis Objectives

The study described in this thesis investigates the best tradeoff between power saving and delay for Nonreal-Time (NRT) traffic. As the NRT traffic is highly irregular and unpredictable. So, the traffic estimation cannot be very accurate and an adaptation of DRX configuration based on this estimation will not result in a very optimum outcome in practice. We propose to avoid the estimation of traffic in NRT applications and instead, a novel simple fashion in the variation of DRX cycle length is proposed.

### Problem formulation

On the basis of changing DRX cycle length for a better trade-off between power saving of the UE and the delay we are going to reply to the following questions in the upcoming chapters:

- Why the approach of changing DRX cycle is used instead of traffic estimation in Nonreal-Time applications?
- How does our proposal function for delay tolerant applications but avoiding the overhead of the messages and admitting the uncertainty in packet arrivals?
- How does our proposal improve the delay in service resumption when there has been a long inactivity without terminating an NRT session?

## 1.2 Study Methodology

To fulfill the objectives of the thesis, we have first of all analyzed the current status of LTE standardization at 3GPP website (<http://www.3gpp.org>) and a set of journal and conference papers. We have then implemented the needed logics into a system level simulator to perform a large set of simulations and analysis over a wide range of parameters setting. The useful results obtained with extensive analytical and simulation work have been then processed and post-processed to find the average behavior of the system.

### 1.2.1 The Simulator

All the simulation studies performed in this thesis is performed with the help of a MATLAB system level simulator expressly developed for the purpose.

## 1.3 Thesis Outlines

The following chapters of the thesis are organized in this way:

- Chapter 2 provides a description of LTE system, the main purposes of the project, the actual specification status and implementation. The main functionalities and characteristics closely involved in the thesis analysis are also explained in detail.
- Chapter 3 represents the existing DRX mechanism in Long Term Evolution (LTE) system. Different parameters of DRX mechanism are put in detail in this chapter.
- Chapter 4 explains the proposed DRX mechanism extensively showing the difference between the existing system
- Chapter 5 describes the analytical model for both existing and proposed scheme. The analytical model elaborately derive the power consumption and delay for both the scheme.
- Chapter 6 shows the simulation result based on the analytical model to validate the proposed scheme. The assumptions for the simulation is described briefly in this chapter.
- Chapter 7 summarizes the report conclusions indication future works.



# Long Term Evolution (LTE)

---

The pervasiveness of the present-day broadband cabled services has made the Internet generation used to high-speed connections and to a whole new set of services usually available exclusively from fixed locations. However, mobile broadband is currently becoming a reality with third generation (3G) technologies.

During the Radio Access Networks (RAN) Future Workshop, it has become clear that 3G long-term evolution has to meet this future services demand, with the constraint to remain competitive for a long time frame i.e. coming decades. A consistent amount of new technologies, like Orthogonal Frequency Division Multiplexing (OFDM) with flexible and broader Radio Frequency (RF), linked with enhancements in both Universal Terrestrial Radio Access Network (UTRAN) architecture and UTRA radio interface were presented as candidates to fulfill this purpose. The main justifications for this evolution path reside in the constant increase of customer utilization of new and traffic-consuming services: people can already successfully browse the Internet, manage emails, send and receive audio-visual contents with High Speed Data Access (HSPA) enabled devices, like smartphones, PDAs, notebook, dongles, but more and more services with higher data rate, low latency and availability are approaching the mobile world.

The starting point of Long Term Evolution (LTE) was fixed when 3rd Generation Partnership Project (3GPP), in the 3GPP Technical Specifications Group (TSG) RAN #26 meeting, approved the study item description on “Evolved UTRA and UTRAN”. LTE performances and technologies have been evaluated with a number of so called checkpoints and the final results agreed on during 3GPP plenary sessions in May 2007 in South Korea.

The goal of LTE is to provide a high-data-rate, low-latency and packet-optimized radio access technology supporting flexible bandwidth deployments. In parallel, new network architecture is designed with the goal to support packet-switched traffic with seamless mobility, quality of service and minimal latency.

## 2.1 LTE System Attributes

The air-interface related attributes of the LTE system are summarized in Table 2.1.

Bandwidth		1.25–20 MHz
Duplexing		FDD, TDD, half-duplex FDD
Mobility		350 km/h
Multiple access	Downlink	OFDMA
	Uplink	SC-FDMA
MIMO	Downlink	2×2, 4×2, 4×4
	Uplink	1×2, 1×4
Peak data rate in 20 MHz	Downlink	173 and 326 Mb/s for 2×2 and 4×4 MIMO, respectively
	Uplink	86 Mb/s with 1×2 antenna configuration
Modulation		QPSK, 16-QAM and 64-QAM
Channel coding		Turbo code
Other techniques		Channel sensitive scheduling, Link adaptation, power control, ICIC and hybrid ARQ

**Table 2.1** LTE System Attributes

The system supports flexible bandwidths thanks to OFDMA and SC-FDMA access schemes. In addition to FDD (frequency division duplexing) and TDD (time division duplexing), half duplex FDD is allowed to support low cost UEs. Unlike FDD, in half-duplex FDD operation a UE is not required to transmit and receive at the same time. This avoids the need for a costly duplexer in the UE. The system is primarily optimized for low speeds up to 15 km/h. However, the system specifications allow mobility support in excess of 350 km/h with some performance degradation. The uplink access is based on single

carrier frequency division multiple access (SC-FDMA) that promises increased uplink coverage due to low peak-to-average power ratio (PAPR) relative to OFDMA. The system supports downlink peak data rates of 326 Mb/s with 4×4 MIMO (multiple input multiple output) within 20 MHz bandwidth. Since uplink MIMO is not employed in the first release of the LTE standard, the uplink peak data rates are limited to 86 Mb/s within 20 MHz bandwidth.

## 2.2 LTE Network Structure

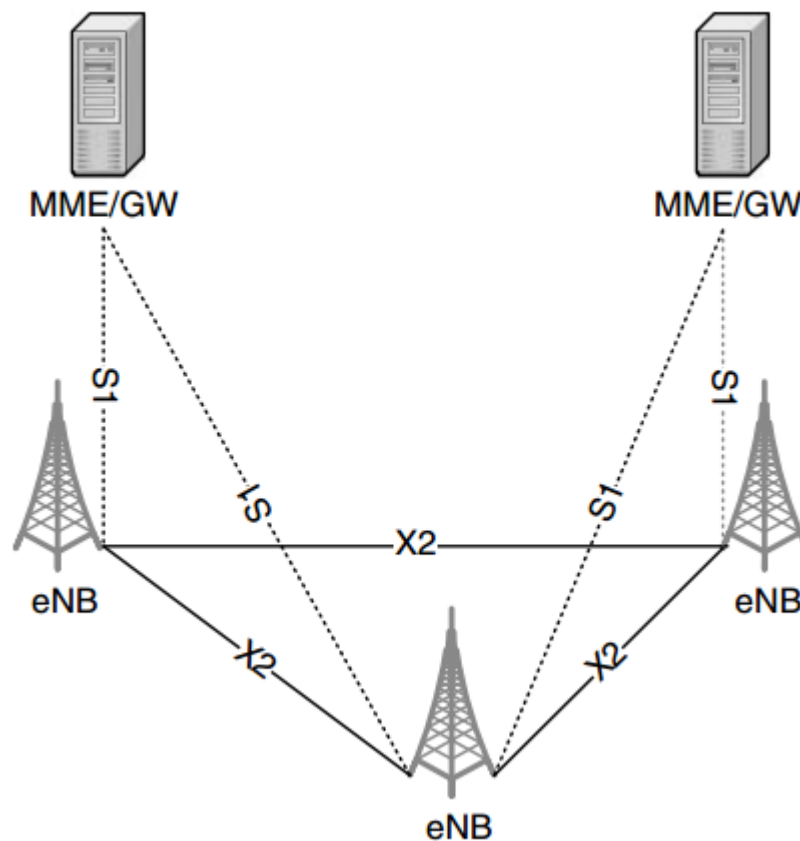


**Figure 2.1.** LTE Network Structure

All the network interfaces are based on IP protocols. The eNBs are interconnected by means of an X2 interface and to the MME/GW entity by means of an S1 interface as shown in Figure 2.1. The S1 interface supports a many-to-many relationship between MME/GW and eNBs.

The functional split between eNB and MME/GW is shown in Figure 2.2. Two logical gateway entities namely the serving gateway (S-GW) and the packet data network gateway (P-GW) are defined. The S-GW acts as a local mobility anchor forwarding and receiving packets to and from the eNB serving the UE. The P-GW interfaces with external packet data networks (PDNs) such as the Internet and the IMS. The P-GW also performs several IP functions such as address allocation, policy enforcement, packet filtering and routing.

The user plane protocol stack is given in Figure 2.3. We note that packet data convergence protocol (PDCP) and radio link control (RLC) layers traditionally terminated in RNC on the network side are now terminated in eNB.

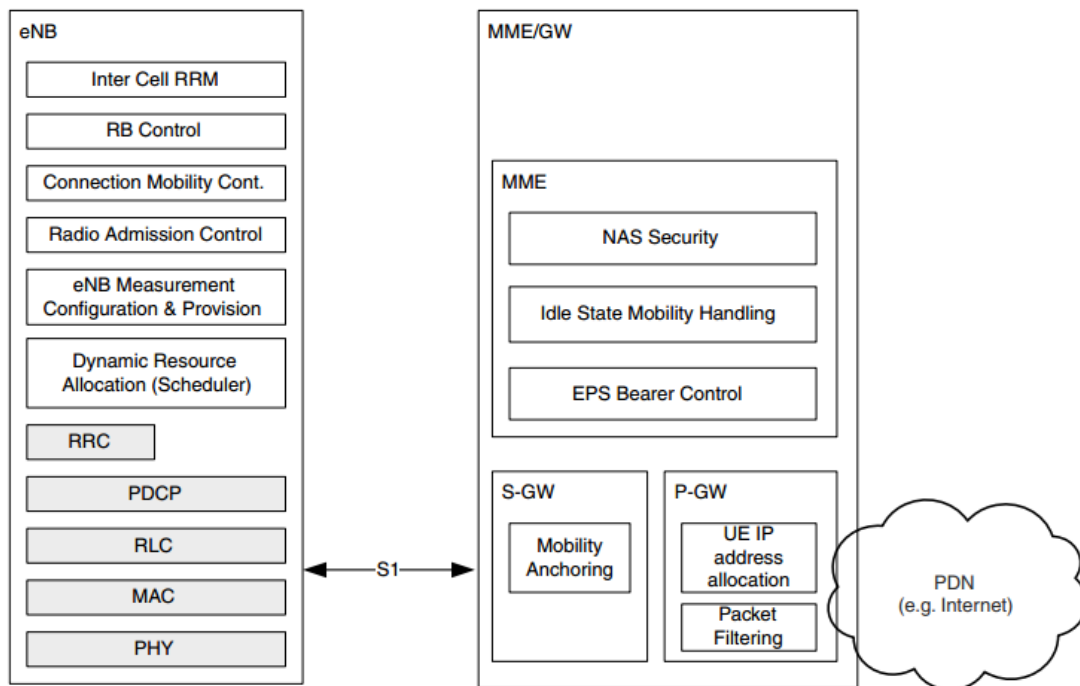


**Figure 2.2.** Functional split between eNB and MME/GW.

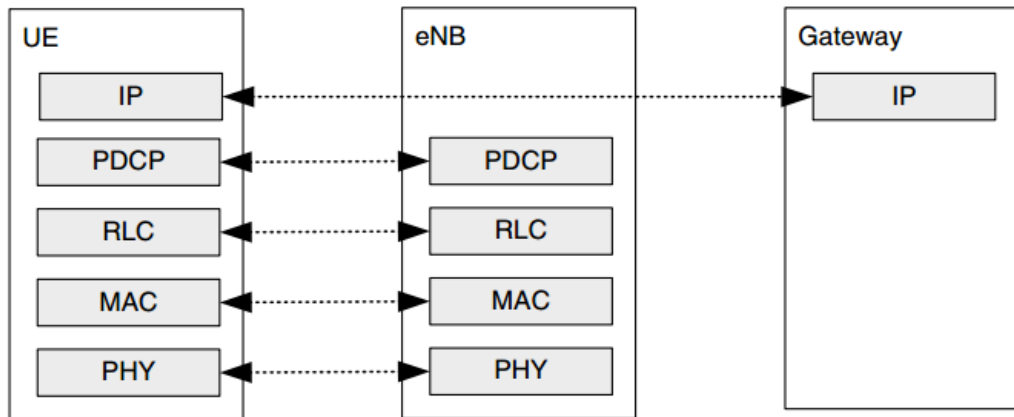


**Figure 2.3.** User Plane Protocol.

Figure 2.4 shows the control plane protocol stack. We note that RRC functionality traditionally implemented in RNC is now incorporated into eNB. The RLC and MAC layers perform the same functions as they do for the user plane. The functions performed by the RRC include system information broadcast, paging, radio bearer control, RRC connection management, mobility functions and UE measurement reporting and control. The non-access stratum (NAS) protocol terminated in the MME on the network side and at the UE on the terminal side performs functions such as EPS (evolved packet system) bearer management, authentication and security control, etc.

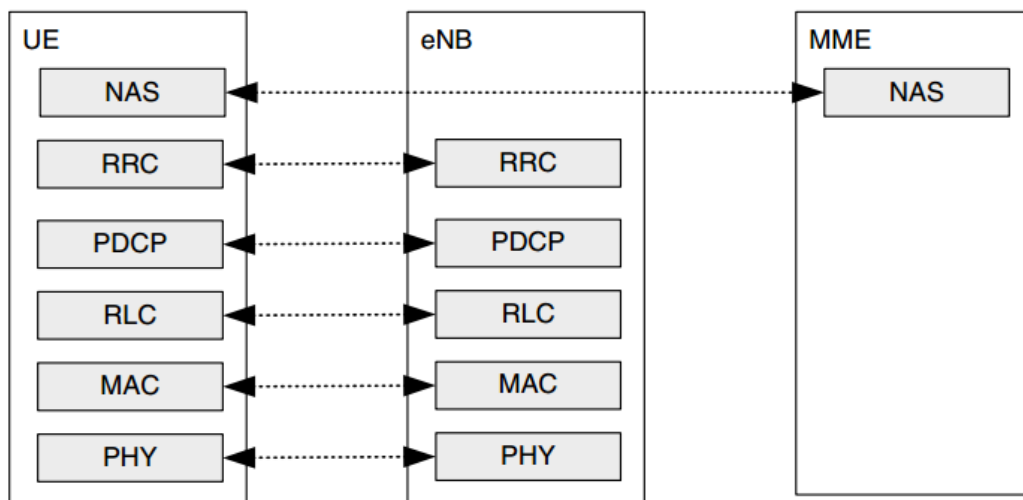


**Figure 2.4.** Control Panel Protocol Stack.

### 2.2.1 Layer 2 Structure

The layer 2 of LTE consists of three sublayers namely medium access control, radio link control (RLC) and packet data convergence protocol (PDCP). The service access point (SAP) between the physical (PHY) layer and the MAC sublayer provide the transport channels while the SAP between the MAC and RLC sublayers provide the logical channels. The MAC sublayer performs multiplexing of logical channels on to the transport channels. The downlink and uplink layer 2 structures are given in Figures 2.5 and 2.6 respectively.

The difference between downlink and uplink structures is that in the downlink, the MAC sublayer also handles the priority among UEs in addition to priority handling among the logical channels of a single UE. The other functions performed by the MAC sublayers in both downlink and uplink include mapping between the logical and the transport channels, multiplexing of RLC packet data units (PDU), padding, transport format selection and hybrid ARQ (HARQ).

The main services and functions of the RLC sublayers include segmentation, ARQ in-sequence delivery and duplicate detection, etc. The in-sequence delivery of upper layer PDUs is not guaranteed at handover. The reliability of RLC can be configured to either acknowledge mode (AM) or un-acknowledge mode (UM) transfers. The UM mode can be used for radio bearers that can tolerate some loss. In AM mode, ARQ functionality of RLC retransmits transport blocks that fail recovery by HARQ. The recovery at HARQ may fail due to hybrid ARQ NACK to ACK error or because the maximum number of retransmission attempts is reached. In this case, the relevant transmitting ARQ entities are notified and potential retransmissions and re-segmentation can be initiated.

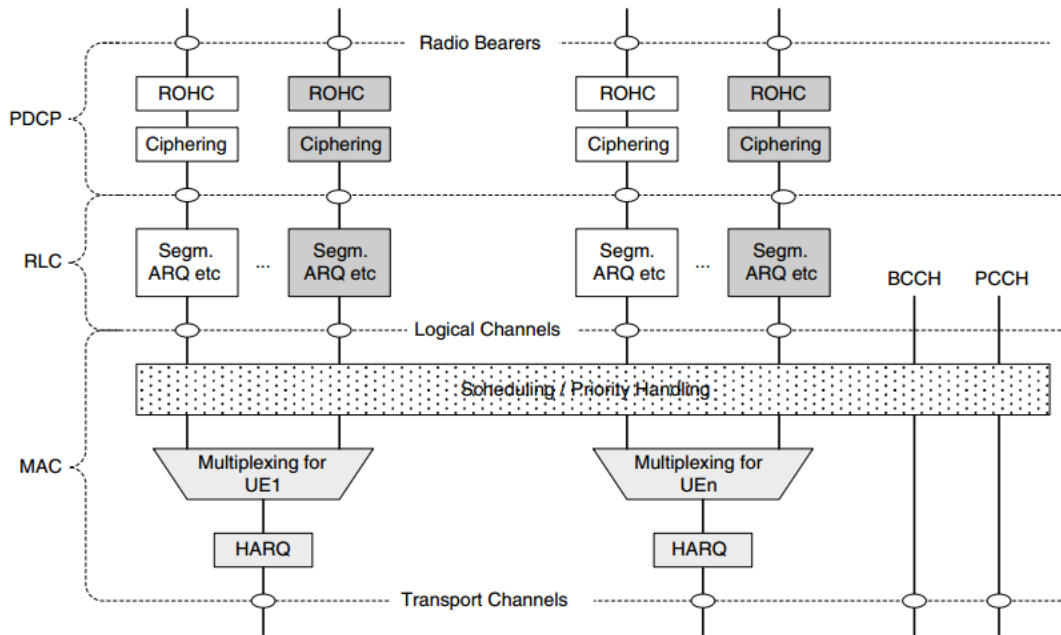


Figure 2.5. Downlink Layer 2 Structure.

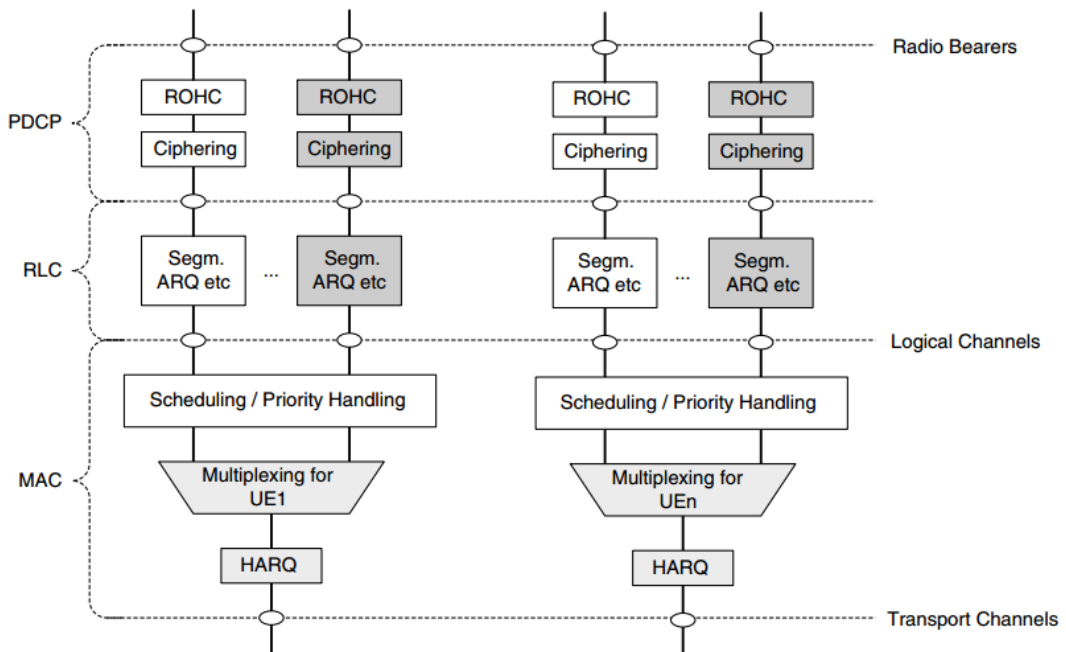


Figure 2.6. Uplink Layer 2 Structure.

## 2.2.2 Radio Resource Control (RRC) States

3GPP specifies two radio resource control states for UE, and related specific protocols to handle UEs in each state:

### **RRC\_IDLE**

UEs in RRC\_IDLE state show sporadic activity that mainly involves cell selection and reselection: UE chooses the cell basing its decision on priority of each applicable frequency of each RAT, radio channel quality cell status (avoids barred or reserved cells). In RRC\_IDLE the UE listens to paging channel too, receiving informations about incoming calls, and system parameters specified by E-UTRAN that assist in the cell selection process.

### **RRC\_CONNECTED**

UEs in RRC\_CONNECTED state have allocated radio resources in shared data channels, specified by dedicated signaling performed via control channels. Also, in this state, the UE periodically reports downlink channel quality to eNB, as well as neighboring cells information including cells using other frequencies or RATs.



### Existing DRX Mechanism

---

In order to save battery power and prolong battery life, the UE may periodically switch off the receiver circuitry. This is referred to as Discontinuous Reception (DRX). A periodic cycle is defined that includes a continuous active period and then a continuous inactive period for the UE. This cycle is called DRX cycle. The power saving occurs during the inactive period. DRX can be applied in both the RRC\_CONNECTED state and the RRC\_IDLE state. The length of the DRX cycle in the RRC\_CONNECTED state is made, at the maximum, equal to the length of the DRX cycle in the RRC\_IDLE state. The maximum possible length of the DRX cycle is 256 radio frames for both the RRC\_IDLE and the RRC\_CONNECTED state.

#### 3.1 DRX in the RRC\_IDLE State

In the RRC\_IDLE state, the UE wakes up once in every DRX cycle and looks for a paging message. The active period of the DRX cycle has one Paging Occasion (PO). Thus, the DRX cycle is the same as the paging cycle for a UE in the RRC\_IDLE state. After the active period of the DRX cycle, the UE exercises DRX (i.e., it turns off the receiver circuitry to save power).

### 3.2 DRX in the RRC\_CONNECTED State

In the RRC\_CONNECTED state, the eNodeB can optionally configure the DRX operation. The RRC layer at eNodeB configures DRX by sending the DRX-Config IE. If DRX is not configured, the UE monitors PDCCH continuously in order to find allocations for downlink or uplink transmission. When DRX is configured, the eNodeB specifies a DRX cycle consists of an “On Duration” at the beginning of the cycle as shown in the figure 3.1. In the rest period of the DRX cycle, the UE exercises RX (i.e., it turns off its receiver circuitry to save power). The UE monitors the PDCCH during On Duration and the UE pauses downlink reception during the DRX period.

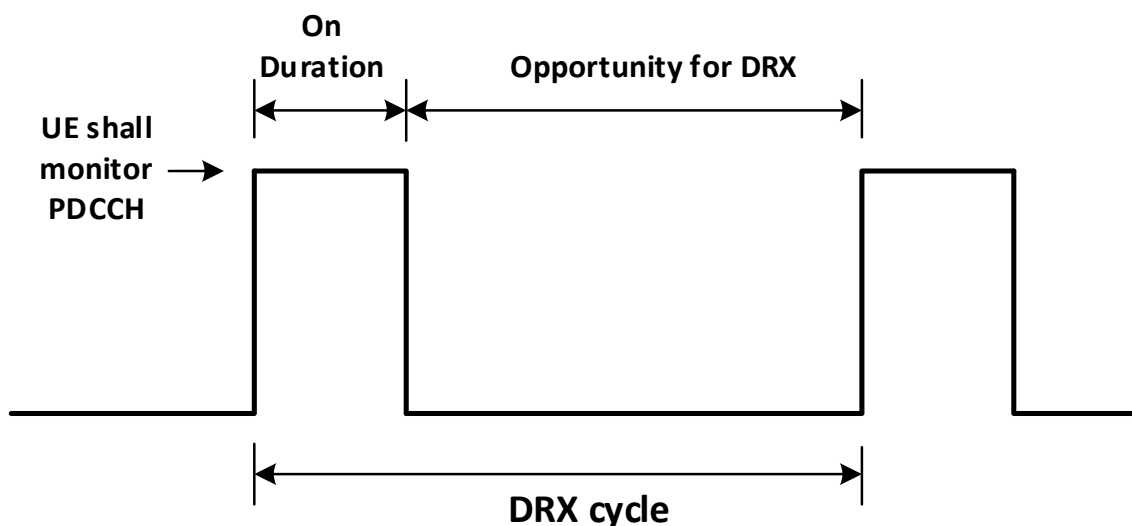


**Figure 3.1** On Duration and DRX period in DRX Cycle

The On Duration Timer field in the DRX-Config IE specifies the length of the On Duration in the number of subframes. It can specify 1, 2, 3, 4, 5, 6, 8, 10, 20, 30, 40, 50, 60, 80, 100 or 200 subframes.

### 3.2.1 Configuration of the DRX Cycle

Two types of DRX cycle are defined-

#### 1. Long DRX Cycle:

The long DRX cycle allows increased power saving although it reduces the frequency of opportunities for scheduling via PDCCH.

#### 2. Short DRX Cycle:

The short DRX cycle is optional. It is used only when there are significant chances of scheduling and the DRX cycle is used otherwise. The short DRX cycle is suitable when there are transmissions of small data at short but regular intervals, for example, VoIP. If the DRX cycle is configured, the UE initiates DRX operation with short DRX cycles, but transitions to long DRX cycle at the expiry of a timer. On the other hand, if the short DRX cycle is not configured, the UE initiates a DRX operation with long DRX cycles.

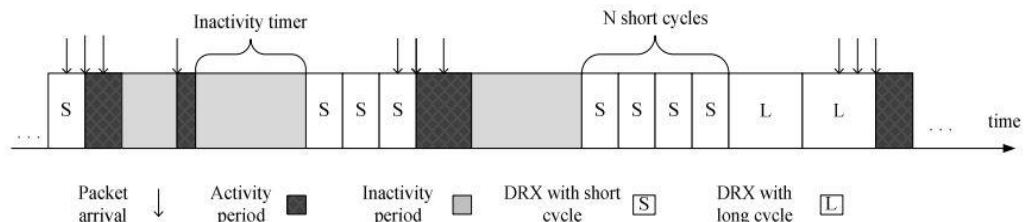


**Figure 3.2** Total DRX Cycles with short and long cycles

If the short DRX cycle is configured the DRX-Config IE includes the short DRX IE. The short DRX IE includes the short DRX-Cycle field, which specifies the length of the short DRX cycle in the number of subframes. It can be 2, 5, 8, 10, 16, 20, 32, 40, 64, 128, 160, 256, 320, 512 or 640 subframes. When the UE initiates DRX with short DRX cycles, it starts a timer called the DRXShortCycleTimer and keeps on going through short DRX cycles one after another until the DRXShortCycleTimer expires. Once the DRXShortCycleTimer expires, the UE initiates long DRX cycles in order to save more battery power. The ShortDRX IE includes the DRXShortCycleTimer field, which specifies the length of the DRXShortCycleTimer in terms of multiples of the

ShortDRX Cycle. The value of the DRXShortCycleTimer can be any integer up to 16. The DRX-Config IE also includes the Long DRX-CycleStartOffset IE, which specifies the values for the following fields.

1. **Long DRX Cycle:** The field specifies the length of the long DRX cycle in the number of subframes. It can be 10, 20, 32, 40, 64, 80, 128, 160, 256, 320, 512, 640, 1024, 1280, 2048 or 2560 subframes. When the short DRX cycle is configured, the value of the Long DRX cycle is chosen such that it becomes a multiple of the Short DRX Cycle.
2. **DRX Start Offset:** This field specifies the particular radio frame and subframe in which the long or short DRX cycle begins. The radio frame and subframe that initiate the long or short DRX cycle are determined by satisfying the following relations-
  - **Long DRX Cycle:** DRX Start Offset =  $[(\text{SFN} \times 10) + (\text{subframe number initiating long DRX cycle})] \bmod \text{LongDRX-Cycle}$ .
  - **Short DRX Cycle:** DRX Start Offset mod ShortDRX-Cycle =  $[(\text{SFN} \times 10) + (\text{subframe number initiating short DRX cycle})] \bmod \text{ShortDRX-Cycle}$ .

### 3.2.2 Continuous Reception and Resumption of DRX

If the UE detects any scheduling while it is monitoring the PDCCH during an on duration, the UE stops the DRX operation, begins continuous reception, and starts a timer called the DRX-Inactivity Timer. The UE maintains continuous reception with no DRX cycle until the DRX-Inactivity Timer expires. If the UE receives any scheduling again on the PDCCH while the DRX-Inactivity Timer is running, the UE restarts the DRX-Inactivity Timer. Once the DRX-Inactivity Timer expires, the UE immediately initiates a short DRX cycle provided that the short DRX cycle is configured. If the short DRX is not configured, then the UE initiates a long DRX cycle instead. The DRX-Config IE includes the DRX-Inactivity Timer field, which specifies the length of the DRX-Inactivity Timer in the number of subframes. It can be 1, 2, 3, 4, 5, 6, 8, 10, 20, 30, 40, 50, 60, 80, 100, 200, 300, 500, 750, 1280, 1920 or 2560 subframes.

Alternatively, the eNodeB can send an explicit command by including the DRX command MAC control element in the MAC PDU during continuous reception. Then the UE initiates a short DRX cycle provided that the short DRX cycle is configured. Again, if the short DRX cycle is not configured, the UE initiates a long DRX cycle instead.

### 3.2.3 HARQ During DRX

HARQ operation is independent of DRX operation. The UE wakes up from sleeping state to monitor the PDCCH for possible HARQ retransmissions and ACK/NAK signaling on OHICH and to transmit HARQ feedbacks when they are due. Each HARQ process expects HARQ round trip time (HARQ RTT) between the transmission and the retransmission of a transport block when the decoding fails. The HARQ RTT is estimated as 8 ms. Therefore, in case of downlink, the HARQ process at the UE maintains a HARQ RTT timer to allow the UE to sleep during the HARQ RTT. The HARQ RTT timer is set to 8 ms.

If the DRX operation is configured, then the UE pauses the monitoring of the PDCCH for a certain period. If decoding a downlink transport block fails, the UE still pauses the monitoring of the PDCCH but for the HARQ RTT period assuming the retransmission of the transport block might take place after the HARQ RTT. Of course, the UE can pause the monitoring of the PDCCH at times only if any other schedule does not come up for monitoring the PDCCH.

When the HARQ RTT timer indicates that the HARQ RTT is over, the UE starts monitoring the PDCCH for retransmission. At this moment, the UE monitors the PDCCH for a maximum period specified by the DRX-RetransmissionTimer. The DRX-Config IE includes the DRX-RetransmissionTimer field, which gives the length of the DRX-RetransmissionTimer in the number of subframes. It can specify 1, 2, 4, 6, 8, 16, 24 or 33 subframes. Also, the UE does not enter the DRX when uplink HARQ is due.

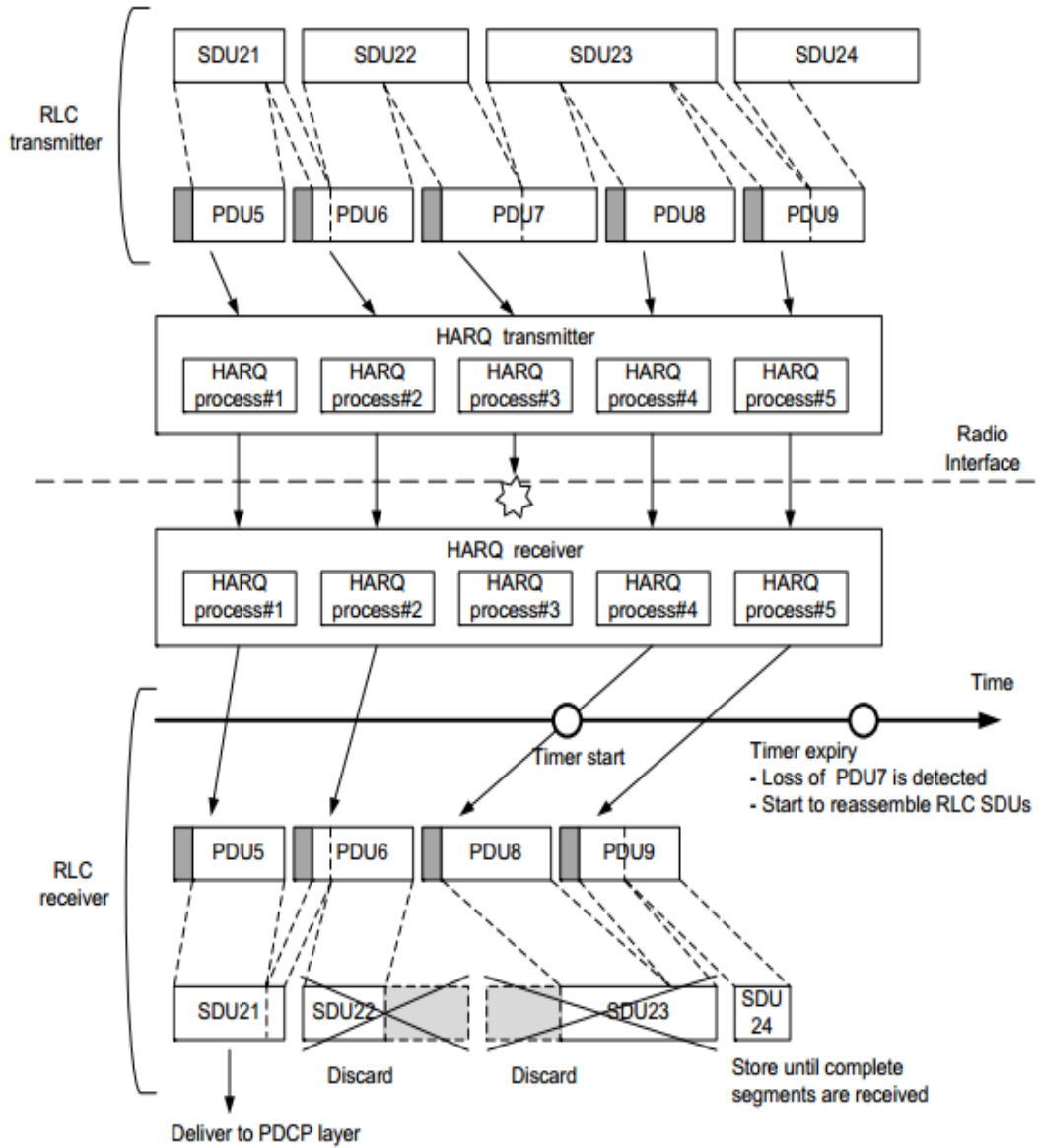


**Figure 3.3** PDU Loss Detection with HARQ Recording

### 3.2.4 Active Time

The active time refers to the duration in which the UE is awake and it monitors PDCCH. Thus, it includes the following durations:

1. On duration in the beginning of the DRX-Cycle.
2. During the data transfer and the DRX-InactivityTimer period after the detection of scheduling on the PDCCH.
3. When the downlink HARQ retransmission is expected and when the uplink HARQ retransmission is due.
4. If the UE has sent a scheduling request.
5. A random access process is in progress and the contention resolution time is running.

While the UE is not in active time, it does not perform any uplink retransmission including of the PUCCH and the SRS.

### 3.3 Depictment of All DRX States

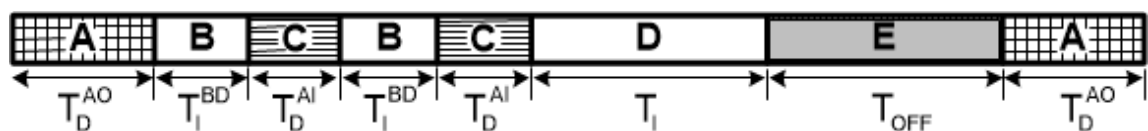


**Figure 3.4** States associated with DRX

The activities with regard to DRX are exemplified in Fig. 3.4.

- State A indicates ordinary data transfer and  $T_D^{AO}$  represents its duration. State B indicates running inactivity timer at the end of ordinary data transfer and  $T_I^{BD}$  represents its duration.
- In state B, the inactivity timer is reset before it expires because of the arrival of a packet. It is uncertain how many times the inactivity timer may be reset as such and how long it would run before getting reset.

- State C indicates data transfer after state B and  $T_D^{AI}$  represents the duration of state C. After every state C, the inactivity timer is restarted.  $N_I^D$  represents how many times the inactivity timer is restarted.
- State D indicates running inactivity timer when the timer can run up to its expiry with no packet arrivals.  $T_I$  represents the whole duration of the inactivity timer.
- State E indicates running DRX cycles continuously after the expiry of the inactivity timer. We assume that there can be N number of short cycles at the maximum. After these short cycles, long cycles start running.  $T_S$  and  $T_L$  represent the length of short and long DRX cycles, respectively. DRX operation is terminated because of the arrival of packets.  $T_{OFF}$  represents the duration of state E.

The data transfer after state E is actually the ordinary data transfer and so, it is shown as state A. The notations and states, shown in this section, will be used in the next chapters.



---

### Proposed DRX Scheme

---

We propose a novel way to vary the DRX cycle length such that it improves the power saving while increasing the delay of NRT traffic within permissible limits. Let us assume that  $E[D_{RT}]$  and  $E[D_{NRT}]$  represent mean total delay for RT and NRT traffic, respectively.  $E[D_{RTX}]$  represents the mean delay for RLC AM retransmissions, which occurs only in the case of NRT traffic. The relationship among these delays can be expressed as

$$E[D_{NRT}] = E[D_{RT}] + E[D_{RTX}]. \quad (1)$$

The PDB for NRT traffic is much larger than that of RT traffic because of the delay tolerance of NRT applications. Thus,  $PDB_{NRT} - PDB_{RT} > E[D_{NRT}] - E[D_{RT}]$ , where  $PDB_{NRT}$  and  $PDB_{RT}$  denote PDB for NRT and RT traffic, respectively. So, we obtain

$$PDB_{NRT} - PDB_{RT} = E[D_{NRT}] - E[D_{RT}] + \bar{\zeta} \quad (2)$$

where  $\bar{\zeta}$  can be expressed using (1) as

$$\bar{\zeta} = PDB_{NRT} - PDB_{RT} - E[D_{RTX}]. \quad (3)$$

However,  $PDB_{NRT} - PDB_{RT} = E[D_{NRT}] - E[D_{RT}]$  can be permissible in the system.

Therefore,  $E[D_{NRT}]$  can be allowed to be increased to  $E[D_{NRT}]_{new}$  given by

$$E[D_{NRT}]_{new} = E[D_{NRT}] + \Delta_{NRT} \quad (4)$$

where (2) sets a constraint

$$\Delta_{NRT} \leq \bar{\zeta}. \quad (5)$$

In our proposal,  $E[D_{NRT}]$  is increased purposely to achieve improvement in power saving while satisfying the constraint in (5). We assume M/G/1 system queue. So, the packet arrival follows Poisson process and the inter-arrival times are distributed exponentially.

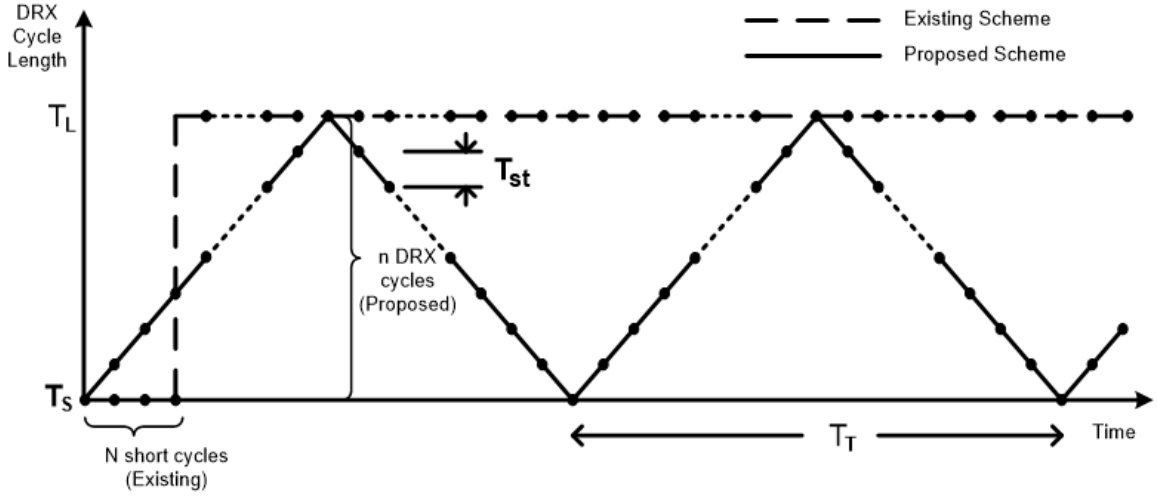


**Figure 4.1** Proposed DRX Mechanism

We assume that the packet arrival rate is  $\lambda$  and the service or transmission rate of the packets is  $\mu$ . The mean transmission time of a packet is  $E[S] = 1/\mu$ . The traffic intensity can be expressed as  $\rho = \lambda/\mu$ . We assume that the system is stable with  $\mu > \lambda$ . In the Poisson process, at any point in time, not necessarily at points of occurrences, the future evolution is independent of the past, i.e.  $P(X > s+t | X > s) = P(X > t)$  for all  $s$  and  $t$  greater or equal to 0. In other words, the Poisson process is memoryless.

If no packet has arrived in  $p$  number of DRX cycles, regardless of the value of  $p$ , the probability that the next DRX cycle cannot complete due to packet arrival is  $P(p+1) = 1 - e^{-\lambda T}$ , where  $T$  represents the length of the next DRX cycle.

If  $T \neq f(p)$ , then  $P(p+1) \neq f(p)$  and this is the case when the DRX cycle length remains constant. This can be regarded as the existing case as it takes on two constant DRX cycle lengths,  $T_s$  and  $T_L$ . In this case,  $P(p+1)$  does not increase with  $p$ . We propose an increase in  $P(p+1)$  with  $p$  for NRT traffic in order to increase the power saving with time. To accomplish it in a simple method, we set  $T = cp$ , where  $c$  is a constant. A simple method can invoke small changes in the associated protocols and help easy and quick implementation. In our proposal, instead of allowing a few short cycles in the beginning, the DRX cycle length keeps increasing from  $T_s$  by a fixed step size  $T_{st}$  until it reaches  $T_L$ . Let us assume that  $n$  number of cycles are taken to reach  $T_L$ . The execution of  $n$  DRX cycles already indicates that there may have been a long inactivity in the session. Our proposal attempts to limit delay in service resumption after a long inactivity.

So, we propose that after  $n$  DRX cycles, the DRX cycle length keeps decreasing from  $T_L$  to  $T_S$  by the same fixed step size  $T_{st}$ . After this decrease, assuming that the service may not resume soon, similar rise in the DRX cycle length is again used. The rise will be followed by a fall like before for the same reason. These repetitions continue leading to a triangular fashion of variation in the DRX cycle length as illustrated in Fig. 4.1. The smooth gradual variation in the DRX cycle length can be expected to match a change in the data traffic to some extent and thus, the estimation of data traffic is avoided. The period of the triangular variation is  $T_T = 2nT_S + n(n + 1)T_{st}$ . The numerical examples in Section VI show that the proposed scheme can satisfy the constraint in (5).

We propose that the eNodeB configures  $T_S$ ,  $T_L$  and  $T_{st}$  using a layer 3 message when a session is set up and for this configuration, the eNodeB considers the operator's choice and an overall estimate of the potential traffic.

In order to evaluate the proposed and existing schemes, we present analytical models using the approach presented in [20], [21].

### 5.1 Different Power Saving Factors

To estimate power saving in DRX analysis, factors have been used in multiple ways. [19] uses percentage power saving as

$$\left( \frac{E[T_{Data}]}{E[T_{Total}]} + \frac{P_{OFF}E[T_{OFF}]}{P_{Data}E[T_{Total}]} \right) \times 100$$

where the power consumption during data transfer and during the period of DRX cycles are denoted as  $P_{Data}$  and  $P_{OFF}$ , respectively.

The expected durations of these two states are denoted as  $E[T_{Data}]$  and  $E[T_{OFF}]$ , respectively.  $E[T_{Total}]$  represents the mean whole duration including data transfer and DRX. [4] uses power saving factor as

$$\frac{E[T_S - T_{ON}] + E[T_L - T_{ON}]}{E[T_{Total}]}$$

where  $E[T_S - T_{ON}]$  and  $E[T_L - T_{ON}]$  represent the expected short and long DRX periods, respectively, excluding the on durations.

[20], [22] use power saving factor as  $\frac{E[T_{OFF}]}{E[T_{Total}]}$  without incorporating any power levels.

## 5.2 Proposed Power Saving Factor

There is a significant difference among the power consumptions during effective data transfer, during the period while the inactivity timer runs looking for data and during DRX.

So, we suggest the incorporation of power levels in power saving estimation but introducing a third power level  $P_{wait}$  denoted as the power consumption while the inactivity timer runs.

Secondly, the power consumption becomes extremely low for DRX cycles of any length [23]-[25]. So, the impact of differences in power consumption for DRX cycles of different lengths and for on durations of different lengths is trivial and so, we ignore such differences for simplicity.

We define the average power consumption as

$$P_{avg} = \frac{P_{Data} \cdot E[T_{Data}] + P_{wait} \cdot E[T_{wait}] + P_{OFF} \cdot E[T_{OFF}]}{E[T_{Total}]} \quad (6)$$

where  $E[T_{wait}]$  denotes the expected duration of running the inactivity timer and

$$E[T_{Total}] = E[T_{Data}] + E[T_{wait}] + E[T_{OFF}]. \quad (7)$$

To better indicate the practical power saving in DRX, we propose that the percentage power consumption is defined as

$$\frac{P_{avg}}{P_{Data}} = \left( \frac{E[T_{Data}]}{E[T_{Total}]} + \frac{P_{wait} E[T_{wait}]}{P_{Data} E[T_{Total}]} + \frac{P_{OFF} E[T_{OFF}]}{P_{Data} E[T_{Total}]} \right) \times 100. \quad (8)$$

To estimate power saving, our thesis computes percentage power consumption using (8) and for this purpose,  $E[T_{OFF}]$ ,  $E[T_{wait}]$  and  $E[T_{Data}]$  are evaluated below for the proposed and existing schemes. We assume M/G/1 queue.

The probability of packet arrival in  $t_1$  duration is

$$\int_0^{t_1} \lambda e^{-\lambda t} dt = 1 - e^{-\lambda t_1}.$$

Thus, the probability of no packet arrival in  $t_1$  duration is

$$1 - \int_0^{t_1} \lambda e^{-\lambda t} dt = e^{-\lambda t_1}.$$

### 5.3 Mean Duration of DRX Operation

The expected duration of continuous DRX operation in the proposed scheme  $E[T_{OFF}]_{prop}$  can be given by

$$E[T_{OFF}]_{prop} = E[T_R] + E[T_F] \quad (9)$$

where  $E[T_R]$  and  $E[T_F]$  represent the mean duration of DRX operation in the rise parts and the fall parts of the triangular periods, respectively.

The probability that no packet arrives in  $j$  number of triangular periods and  $(k-1)$  number of DRX cycles of the rise part of  $(j+1)$  numbered triangular period and thereafter packet arrives in the next DRX cycle (i.e.  $k^{\text{th}}$  cycle of the rise part), can be expressed as

$$\chi_{j,k}^R = e^{-j\lambda T_T} R_k. \quad (10)$$

Here,  $R_k$  is given by

$$R_k = e^{-\delta_{k,R}\lambda} [1 - e^{-\lambda(T_S + kT_{st})}] \quad (11)$$

where  $\delta_{k,R}$  is given by

$$\begin{aligned} \delta_{k,R} &= (T_S + T_{st}) + (T_S + 2T_{st}) + \dots + [T_S + (k-1)T_{st}] \\ &= (k-1)T_S + \frac{k(k-1)T_{st}}{2}. \end{aligned} \quad (12)$$

The whole duration of DRX associated with  $\chi_{j,k}^R$  is given by

$$\begin{aligned} T_{j,k}^R &= jT_T + (T_S + T_{st}) + (T_S + 2T_{st}) + \dots + (T_S + kT_{st}) \\ &= jT_T + kT_S + \frac{k(k+1)T_{st}}{2}. \end{aligned} \quad (13)$$

$E[T_R]$  can be expressed as

$$\begin{aligned}
E[T_R] &= \sum_{j=0}^{\infty} \sum_{k=1}^n \chi_{j,k}^R \cdot T_{j,k}^R \\
&= \sum_{k=1}^n R_k \left[ T_T \sum_{j=0}^{\infty} j e^{-j\lambda T_T} + \left\{ kT_S + \frac{k(k+1)T_{st}}{2} \right\} \sum_{j=0}^{\infty} e^{-j\lambda T_T} \right] \\
&= \frac{e^{-\lambda T_T}}{(1-e^{-\lambda T_T})^2} \left[ T_T \sum_{k=1}^n R_k + (1-e^{-\lambda T_T}) \sum_{k=1}^n R_k \left\{ kT_S + \frac{k(k+1)T_{st}}{2} \right\} \right]. \tag{14}
\end{aligned}$$

Similarly, the probability that no packet arrives in  $j$  number of triangular periods and in the  $T_T/2$  long rise part and  $(k-1)$  number of DRX cycles of the fall part of  $(j+1)$  numbered triangular period and thereafter packet arrives in the next DRX cycle (i.e.  $k^{\text{th}}$  cycle of the fall part), can be expressed as

$$\chi_{j,k}^F = e^{-j\lambda T_T} e^{-\lambda(T_T/2)} F_k. \tag{15}$$

Here,  $F_k$  is given by

$$F_k = e^{-\delta_{k,F}\lambda} \left[ 1 - e^{\lambda\{T_S + (n-k)T_{st}\}} \right] \tag{16}$$

where  $\delta_{k,F}$  is given by

$$\begin{aligned}
\delta_{k,F} &= \{T_S + (n-1)T_{st}\} + \dots + [T_S + \{n - (k-1)\}T_{st}] \\
&= (k-1)T_S + \frac{(2n-k)(k-1)T_{st}}{2}. \tag{17}
\end{aligned}$$

The whole duration of DRX associated with  $\chi_{j,k}^F$  is given by

$$\begin{aligned}
T_{j,k}^F &= jT_T + \frac{T_T}{2} + [T_S + (n-1)T_{st}] + \dots + [T_S + (n-k)T_{st}] \\
&= jT_T + \frac{T_T}{2} + kT_S + T_{st} \left[ nk - \frac{k(k+1)}{2} \right]. \tag{18}
\end{aligned}$$

$E[T_F]$  can be expressed as

$$\begin{aligned}
E[T_F] &= \sum_{j=0}^{\infty} \sum_{k=1}^n \chi_{j,k}^F \cdot T_{j,k}^F \\
&= e^{-\lambda(T_T/2)} \sum_{k=1}^n F_k \left[ T_T \sum_{j=0}^{\infty} j e^{-j\lambda T_T} + \left[ \frac{T_T}{2} + kT_s + T_{st} \left\{ nk - \frac{k(k+1)}{2} \right\} \right] \sum_{j=0}^{\infty} e^{-j\lambda T_T} \right] \\
&= \frac{e^{-\frac{3\lambda T_T}{2}}}{(1-e^{-\lambda T_T})^2} \left[ T_T \sum_{k=1}^n F_k + (1-e^{-\lambda T_T}) \sum_{k=1}^n F_k \left[ \frac{T_T}{2} + kT_s + T_{st} \left\{ nk - \frac{k(k+1)}{2} \right\} \right] \right]. \tag{19}
\end{aligned}$$

$E[T_{OFF}]_{prop}$  can now be determined using (9), (14) and (19). The mean duration of DRX in the existing scheme  $E[T_{OFF}]_{exist}$  is given by

$$E[T_{OFF}]_{exist} = E[T_S] + E[T_L] \tag{20}$$

where  $E[T_S]$  and  $E[T_L]$  represent the mean duration of short and long cycles, respectively.

The probability that  $(i-1)$  number of short cycles occur with no packet arrival and thereafter packet arrives in  $i^{\text{th}}$  short cycle, can be expressed as

$$\chi_i^S = (e^{-\lambda T_s})^{i-1} (1 - e^{-\lambda T_s}). \tag{21}$$

The mean number of short cycles  $E[N_{SC}]$  is given by

$$\begin{aligned}
E[N_{SC}] &= \sum_{i=1}^N i \cdot \chi_i^S = e^{\lambda T_s} (1 - e^{-\lambda T_s}) \sum_{i=1}^N i (e^{-\lambda T_s})^i \\
&= \frac{(1 - e^{-N\lambda T_s})}{(1 - e^{-\lambda T_s})} - N e^{-N\lambda T_s}. \tag{22}
\end{aligned}$$

$E[T_S]$  is given by

$$E[T_S] = T_s E[N_{SC}] = T_s \left[ \frac{(1 - e^{-N\lambda T_s})}{(1 - e^{-\lambda T_s})} - N e^{-N\lambda T_s} \right]. \tag{23}$$



The probability that no packet arrives in  $N$  number of short cycles and  $(j-1)$  number of long cycles and thereafter, packet arrives in  $j^{\text{th}}$  long cycle, can be expressed as

$$\chi_j^L = e^{-N\lambda T_s} (e^{-\lambda T_L})^{j-1} (1 - e^{-\lambda T_L}). \quad (24)$$

So, the mean number of long cycles  $E[N_{LC}]$  is given by

$$\begin{aligned} E[N_{LC}] &= \sum_{j=1}^{\infty} j \chi_j^L = e^{-N\lambda T_s} (1 - e^{-\lambda T_L}) \sum_{j=1}^{\infty} j (e^{-\lambda T_L})^{j-1} \\ &= \frac{e^{-N\lambda T_s}}{1 - e^{-\lambda T_L}}. \end{aligned} \quad (25)$$

$E[T_L]$  is given by

$$E[T_L] = T_L E[N_{LC}] = \frac{T_L e^{-N\lambda T_s}}{1 - e^{-\lambda T_L}}. \quad (26)$$

$E[T_{OFF}]_{exist}$  can now be determined using (20), (23) and (26).

## 5.4 Mean Duration of Running Inactivity Timer

The probability  $P_x$  that the inactivity timer restarts  $x$  times because of packet arrivals and thereafter, the inactivity timer expires once completing  $T_I$ , can be expressed as

$$P_x = (1 - e^{-\lambda T_I})^x e^{-\lambda T_I}. \quad (27)$$

So, the mean number of restart of the inactivity timer  $E[N_I^D]$  is given by

$$\begin{aligned} E[N_I^D] &= \sum_{x=0}^{\infty} x P_x \\ &= e^{-\lambda T_I} \sum_{x=0}^{\infty} x (1 - e^{-\lambda T_I})^x = e^{\lambda T_I} - 1. \end{aligned} \quad (28)$$

As the inactivity timer runs, the occurrences in the scenario are limited to the expiry of the timer (i.e. the occurrences lie only within the range as long as the timer runs). Thus, the truncated exponential distribution can be used for the packet arrivals to estimate  $T_I^{BD}$ .

The truncated exponential distribution can be expressed as

$$\begin{aligned} f(t) &= \frac{\lambda e^{-\lambda t}}{1 - e^{-\lambda T_I}}, \quad 0 \leq t \leq T_I \\ &= 0, \quad t > T_I \end{aligned} \quad (29)$$

$E[T_I^{BD}]$  can be expressed as

$$\begin{aligned} E[T_I^{BD}] &= \int_0^\infty t f(t) dt = \frac{\lambda}{1 - e^{-\lambda T_I}} \int_0^{T_I} t e^{-\lambda t} dt \\ &= \frac{1}{\lambda} - \frac{T_I}{e^{\lambda T_I} - 1}. \end{aligned} \quad (30)$$

The mean duration of running inactivity timer is the summation of the average period in state B and state D. Since the average period in state B is  $E[T_I^{BD}]E[N_I^D]$  and the period in state D is  $T_I$ ,  $E[T_{wait}]$  for both the existing and the proposed methods can be expressed as

$$\begin{aligned} E[T_{wait}] &= E[T_I^{BD}]E[N_I^D] + T_I \\ &= \frac{e^{\lambda T_I} - 1}{\lambda}. \end{aligned} \quad (31)$$

## 5.5 Mean Duration of Data Transfer

The mean duration of data transfer is the summation of the average period in state A and state C. Since  $E[N_I^D]$  is the mean number of restart of the inactivity timer, the mean duration of data transfer  $E[T_{Data}]$  for both the existing and the proposed methods can be given by

$$E[T_{Data}] = E[T_D^{AO}] + E[T_D^{AI}]E[N_I^D]. \quad (32)$$

When a single packet is transmitted, its mean transmission time is  $E[S]=1/\mu$ . The probability of  $m$  number of packet arrivals in this  $1/\mu$  duration  $P_m$  is given by

$$P_m = \frac{e^{-\lambda/\mu} (\lambda/\mu)^m}{m!} = \frac{e^{-\rho} \cdot \rho^m}{m!}. \quad (33)$$

So, the mean number of packet arrivals in  $1/\mu$  duration can be shown as

$$\sum_{m=0}^\infty m P_m = \sum_{m=0}^\infty m \frac{e^{-\rho} \cdot \rho^m}{m!} = \rho. \quad (34)$$

If one packet arrives while the inactivity timer is running, then within its transmission period, additional  $\rho$  number of packets arrive on average. These additional packets require additional  $\rho/\mu$  transmission period in which further  $\rho\lambda/\mu = \rho^2$  number of packets arrive on average. This ideally grows up and the total expected transmission period is given by

$$\begin{aligned} E[T_D^{AI}] &= \frac{1}{\mu} + \frac{\rho}{\mu} + \frac{\rho^2}{\mu} + \frac{\rho^3}{\mu} + \dots \\ &= \frac{1}{\mu} \sum_{k=0}^{\infty} \rho^k = \frac{1}{\mu(1-\rho)}. \end{aligned} \quad (35)$$

$E[T_D^{AO}]$  can be determined similarly. During the DRX period  $E[T_{OFF}]$ ,  $\lambda E[T_{OFF}]$  number of packets arrive. These packets require  $\lambda E[T_{OFF}]/\mu = \rho E[T_{OFF}]$  transmission period. In this period, additional  $\lambda \rho E[T_{OFF}]$  number of packets arrive, which require additional  $\lambda \rho E[T_{OFF}]/\mu = \rho^2 E[T_{OFF}]$  transmission period. Thus,  $E[T_D^{AO}]$  is given by

$$\begin{aligned} E[T_D^{AO}] &= E[T_{OFF}] \{\rho + \rho^2 + \dots\} \\ &= E[T_{OFF}] \sum_{k=1}^{\infty} \rho^k = \frac{\rho}{1-\rho} E[T_{OFF}]. \end{aligned} \quad (36)$$

Using equations (28), (32), (35) and (36),  $E[T_{Data}]$  can be expressed as

$$\begin{aligned} E[T_{Data}] &= \frac{\rho}{1-\rho} E[T_{OFF}] + (e^{\lambda T_I} - 1) \frac{1}{\mu(1-\rho)} \\ &= \frac{\rho}{1-\rho} \left\{ E[T_{OFF}] + \frac{e^{\lambda T_I} - 1}{\lambda} \right\} \\ &= \frac{\rho}{1-\rho} \{ E[T_{OFF}] + E[T_{wait}] \} \end{aligned} \quad (37)$$

$E[T_{Data}]_{exist}$  and  $E[T_{Data}]_{prop}$  can be evaluated for the existing and the proposed methods, respectively, using (9), (20), (31) and (37). Similarly,  $E[T_{Total}]_{exist}$  and  $E[T_{Total}]_{prop}$  can be evaluated for the existing and the proposed methods, respectively, using (7).

## 5.6 Delay Performance

The delay analysis will be different between the cases when the UE is running DRX and when the UE is not running. Let us assume that  $N_Q$  represents the number of packets in the queue but excluding those for whom transmission is ongoing and  $W_Q$  represents the waiting time of a packet from the moment it arrives until its transmission commences. Then Little's formula gives the relationship

$$E[N_Q] = \lambda E[W_Q]. \quad (38)$$

The mean residual service time  $E[R]$  represents the mean service or transmission time of packets currently in transmission when a packet arrives. Since  $\frac{E[N_Q]}{\mu}$  represents the service time of all packets ahead in the queue waiting for service, according to Pollaczek Khintchine formula, the mean wait time in the queue is given by

$$E[W_Q] = E[R] + \frac{E[N_Q]}{\mu}. \quad (39)$$

Using Little's formula, we obtain

$$\begin{aligned} E[W_Q] &= E[R] + \rho E[W_Q] \\ &= \frac{E[R]}{1-\rho}. \end{aligned} \quad (40)$$

But  $E[R]$  has the relationship [26]

$$E[R] = \frac{\lambda E[S^2]}{2}. \quad (41)$$

Using (40), we obtain

$$E[W_Q] = \frac{\lambda E[S^2]}{2(1-\rho)}. \quad (42)$$

While the UE is not in DRX (i.e., in states A, B, C or D), the packet delay can be given by

$$E[D_{N\_DRX}] = E[W_Q] = \frac{\lambda E[S^2]}{2(1-\rho)}. \quad (43)$$

On the other hand, while the UE is running DRX (i.e., in state E), the packet may arrive anytime within the DRX cycle. Then there will be an additional delay  $E[W_D]$  because the

packets are not processed until the particular DRX cycle is over. The overall mean delay  $E[D_{DRX}]$  can be given by

$$E[D_{DRX}] = E[W_Q] + E[W_D]. \quad (44)$$

The Poisson process has time-homogeneity, (i.e. the occurrences are equally likely to happen at all times). Thus, the packet can arrive at any time during the DRX cycle with equal probability and it has to wait for the rest of the DRX cycle for any process to begin. The mean wait time here is equivalent to  $E[R]$ . So,  $E[R]_{prop}$  for either the rise time or the fall time of the proposed method can be expressed as

$$\begin{aligned} E[R]_{prop} &= \frac{1}{n} \left[ \frac{T_s + T_{st}}{2} + \frac{T_s + 2T_{st}}{2} + \dots + \frac{T_s + nT_{st}}{2} \right] \\ &= \frac{2T_s + (n+1)T_{st}}{4}. \end{aligned} \quad (45)$$

Using (40) and (45),  $E[W_D]_{prop}$  can be expressed as

$$E[W_D]_{prop} = \frac{2T_s + (n+1)T_{st}}{4(1-\rho)}. \quad (46)$$

The mean delay in the case of rise time  $E[D_{DRX}]_R$  and fall time  $E[D_{DRX}]_F$  can be expressed using (42), (44) and (46) as

$$\begin{aligned} E[D_{DRX}]_R &= E[D_{DRX}]_F = E[W_Q] + E[W_D]_{prop} \\ &= \frac{\lambda E[S^2]}{2(1-\rho)} + \frac{2T_s + (n+1)T_{st}}{4(1-\rho)}. \end{aligned} \quad (47)$$

Denoting the probability of packet arrival during the rise time and the fall time of the proposed method as  $\gamma_R$  and  $\gamma_F$ , respectively, they can be expressed as

$$\gamma_R = \frac{E[T_R]}{E[T_{Total}]_{prop}} \quad (48)$$

and

$$\gamma_F = \frac{E[T_F]}{E[T_{Total}]_{prop}}. \quad (49)$$

So, the overall packet delay for the proposed method  $E[D_{NRT}]_{prop}$  can be expressed as

$$\begin{aligned} E[D_{NRT}]_{prop} &= (1 - \gamma_R - \gamma_F)E[D_{N\_DRX}] + \gamma_R E[D_{DRX}]_R + \gamma_F E[D_{DRX}]_F \\ &= \frac{1}{2(1-\rho)} \left[ \lambda E[S^2] + (\gamma_R + \gamma_F) \left\{ T_s + \frac{(n+1)T_{st}}{2} \right\} \right]. \end{aligned} \quad (50)$$

Similarly,  $E[W_D]$  can be estimated for the existing method as  $E[W_D]_{exist\_S}$  and  $E[W_D]_{exist\_L}$  for short and long DRX cycles, respectively and they can be expressed as

$$E[W_D]_{exist\_S} = \frac{T_s}{2(1-\rho)} \quad (51)$$

and

$$E[W_D]_{exist\_L} = \frac{T_L}{2(1-\rho)}. \quad (52)$$

Denoting the probability of packet arrival during short cycle and long cycle of the existing method as  $\gamma_s$  and  $\gamma_L$ , respectively, they can be expressed as

$$\gamma_s = \frac{E[T_s]}{E[T_{Total}]_{exist}} \quad (53)$$

and

$$\gamma_L = \frac{E[T_L]}{E[T_{Total}]_{exist}}. \quad (54)$$

The overall packet delay for the existing method  $E[D_{NRT}]_{exist}$  can be expressed as

$$\begin{aligned} E[D_{NRT}]_{exist} &= (1 - \gamma_s - \gamma_L) E[W_Q] + \gamma_s \left[ E[W_Q] + \frac{T_s}{2(1-\rho)} \right] \\ &\quad + \gamma_L \left[ E[W_Q] + \frac{T_L}{2(1-\rho)} \right] \\ &= \frac{1}{2(1-\rho)} \{ \lambda E[S^2] + \gamma_s T_s + \gamma_L T_L \}. \end{aligned} \quad (55)$$

The mean delay in service resumption after a long inactivity, without terminating the session, can be estimated as  $E[W_D]$ . So, it will be  $E[W_D]_{prop}$  and  $E[W_D]_{exist\_L}$  for the proposed and existing methods, given by (46) and (52), respectively.

---

# Simulation Results

---

To validate our proposed scheme we have simulate the proposed and the existing system. The performance was evaluated for the proposed and existing methods numerically using the analytical models.

### 6.1 Simulation Assumptions

The assumptions for the simulations are-

- [7] gives the typical values of PDB as  $PDB_{RT} = 100 \text{ ms}$  and  $PDB_{NRT} = 300 \text{ ms}$ .
- As shown in Section II, the overall delay due to RLC retransmissions can be estimated as the summation of the reordering timer value and RTT. The RTT is commonly estimated as 8 ms [1].
- The reordering timer value can take on values between 0 ms and 100 ms with 5 ms gaps or values between 100 ms and 200 ms with 10 ms gaps [18]. Assuming all reordering timer values in the specification equally likely to occur, we set the mean reordering timer value as 85 ms.

So, the mean overall delay due to RLC retransmissions  $E[D_{RTX}]$  is set to 93 ms. Using (3),  $\bar{\zeta}$  can be estimated as 107 ms.

So, the constraint in (5) is  $\Delta_{NRT} \leq \mathbf{107 \text{ ms}}$ .

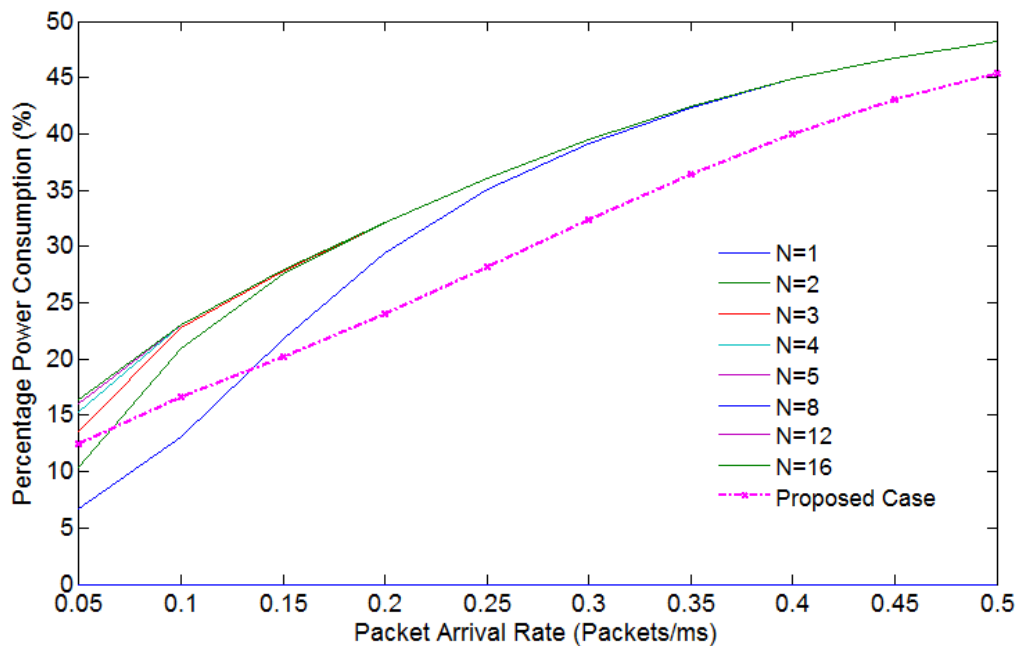
The performance evaluation was performed for three different cases for which the assumptions are shown in Table 1. The values of  $T_I$ ,  $T_S$  and  $T_L$  in Table 1 comply with the permissible values in [18]. The values of  $P_{Data}$ ,  $P_{wait}$  and  $P_{OFF}$  in Table 1 follow the UE power consumption model used in [23]-[25].

Parameter	Case 1	Case 2	Case 3
$T_S$	20 ms	10 ms	10 ms
$T_L$	320 ms	640 ms	40 ms
$T_{st}$	20 ms	30 ms	10 ms
n	15	21	3
$T_I$	10 ms		
N	1, 2, 3, 4, 5, 8, 12 and 16		
$P_{Data}$	500 mW		
$P_{wait}$	255 mW		
$P_{OFF}$	11 mW		
Packet arrival rate ( $\lambda$ )	0.05 to 0.5 packets/ms		
Service rate ( $\mu$ )	100 packets/ms		

**Table 6.1** Simulation assumptions.

## 6.2 Simulation Output

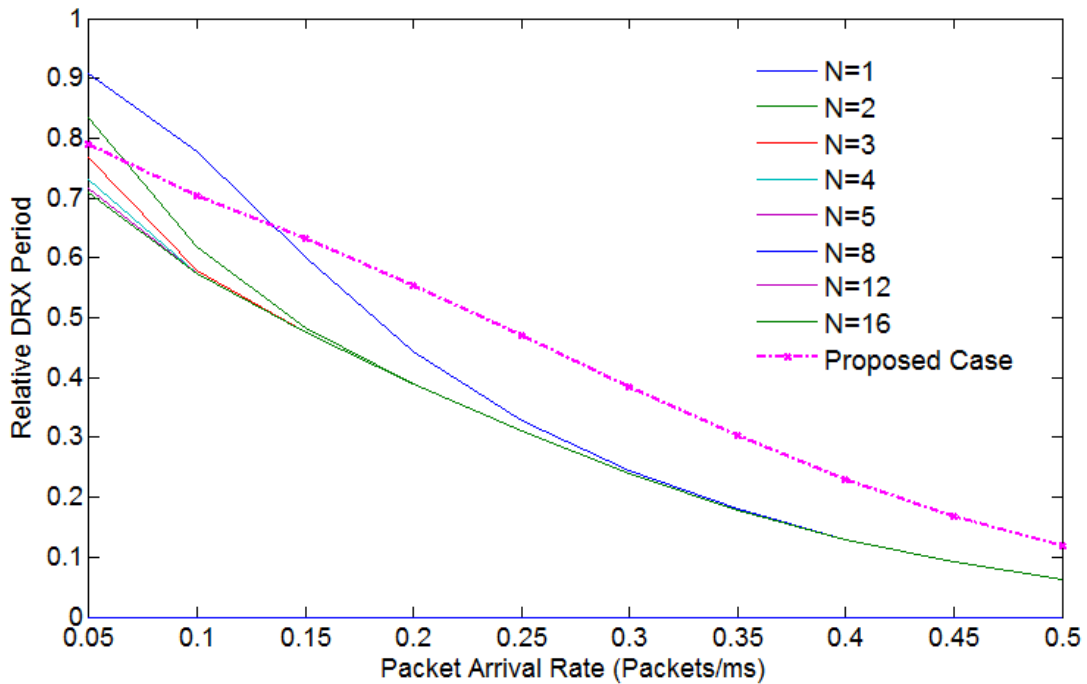
Figure 6.1 shows that the percentage power consumption, in case 1, has significantly improved in the proposed method compared to the existing method for almost all values of packet arrival rate  $\lambda$ .



**Fig. 6.1** Percentage power consumption vs. packet arrival rate (case 1)

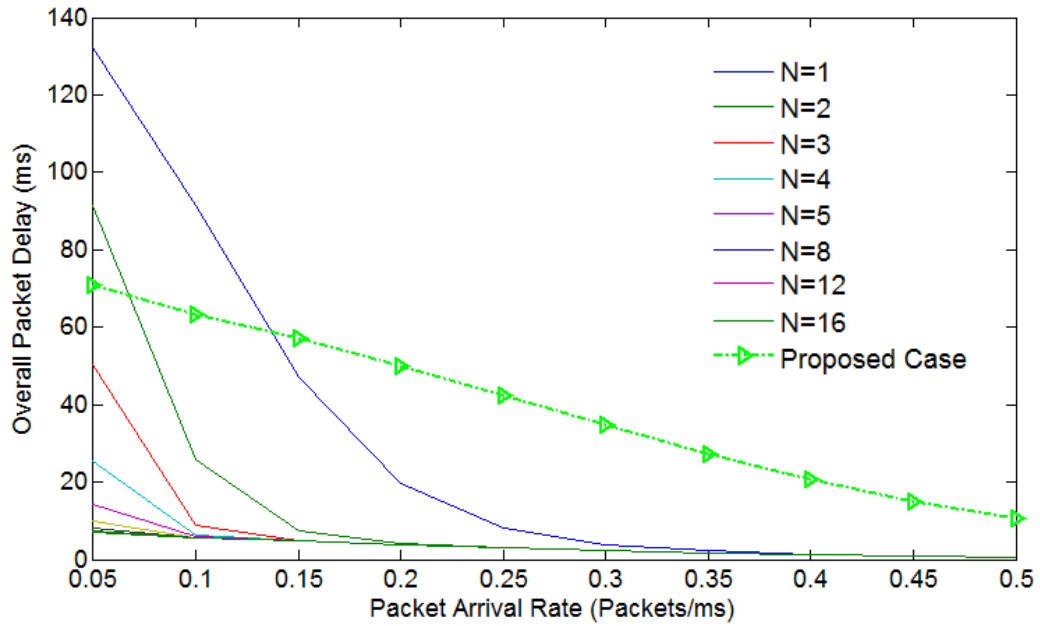


Figure 6.2 shows the relative DRX period  $\frac{E[T_{OFF}]}{E[T_{Total}]}$  indicating that the proposed method exhibits much longer DRX period in most cases. However, the existing method with  $N = 1$  has better power saving for a significant range of  $\lambda$ . The power saving is also little better for  $N = 2$  but for a very limited range of  $\lambda$ .



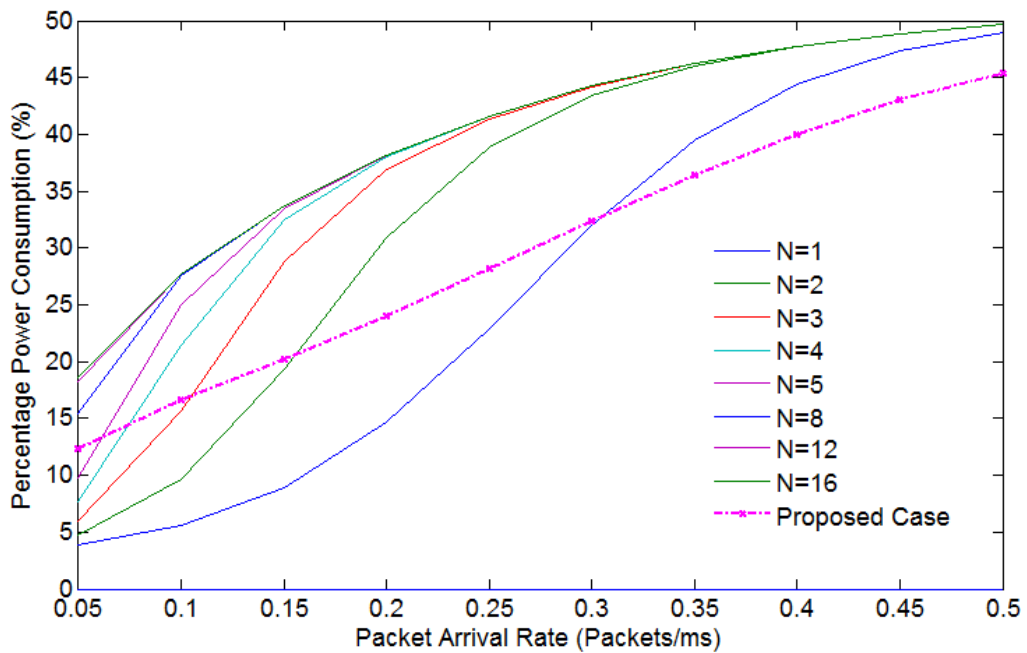
**Fig. 6.2** Relative DRX period  $\left(\frac{E[T_{OFF}]}{E[T_{Total}]}\right)$  vs. packet arrival rate (case 1)

[10] shows that short DRX cycles are very effective in reducing latency. This is also demonstrated by Fig. 6.3 in which the delay takes on the best values in the existing method with very high number of short DRX cycles. We use this delay performance as the benchmark to evaluate  $\Delta_{NRT}$  for other cases. Compared to this benchmark, the proposed method has roughly 60 ms longer delay for  $\lambda = 0.05$  packets/ms and so, we assume  $\Delta_{NRT} = 60$  ms. This increase in delay can be tolerable because  $\Delta_{NRT} \leq 107$  ms. Conversely, the existing method with  $N = 1$ , has almost 120 ms longer delay for  $\lambda = 0.05$  packets/ms and this increased delay may not be acceptable because  $\Delta_{NRT} > 107$  ms. Thus, repudiating the existing method with  $N = 1$ , the proposed method remains the best in performance.



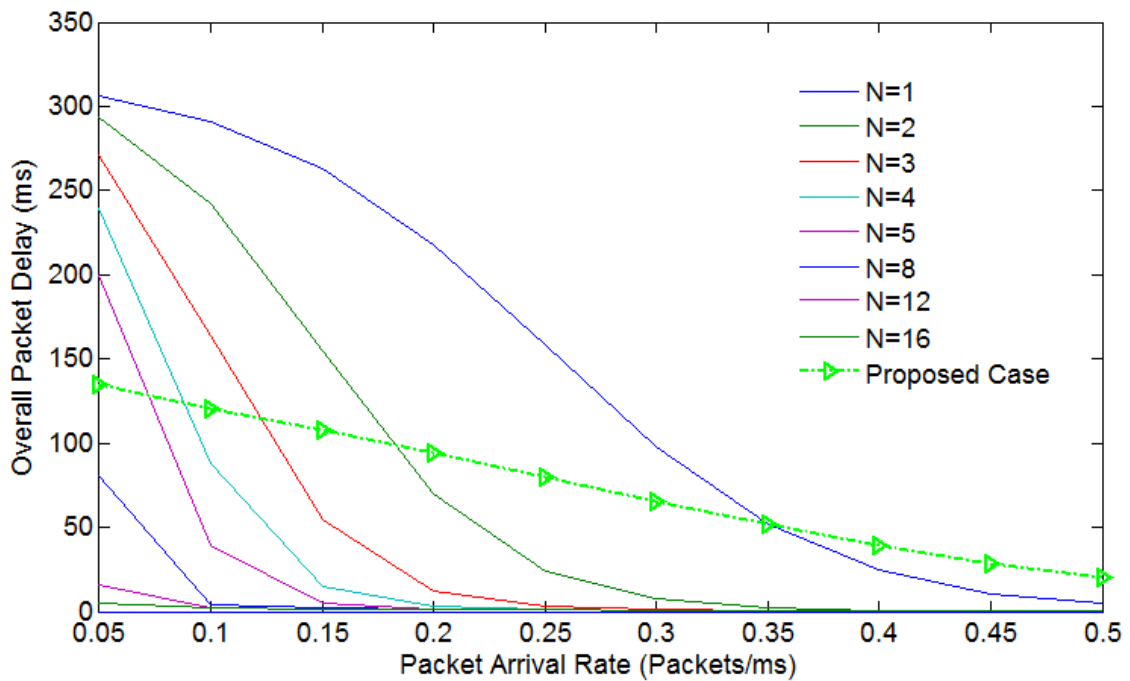
**Fig. 6.3** Overall packet delay vs. packet arrival rate (case 1)

Figure 6.4 shows that the percentage power consumption, in case 2, becomes much better in the proposed method for a significant range of  $\lambda$ , except when the existing method has  $N = 1, 2$  and  $3$ . The power saving is little better in the existing methods with  $N = 4$  and  $5$ , but for a very limited range of  $\lambda$ .



**Fig. 6.4** Percentage power consumption vs. packet arrival rate (case 2)

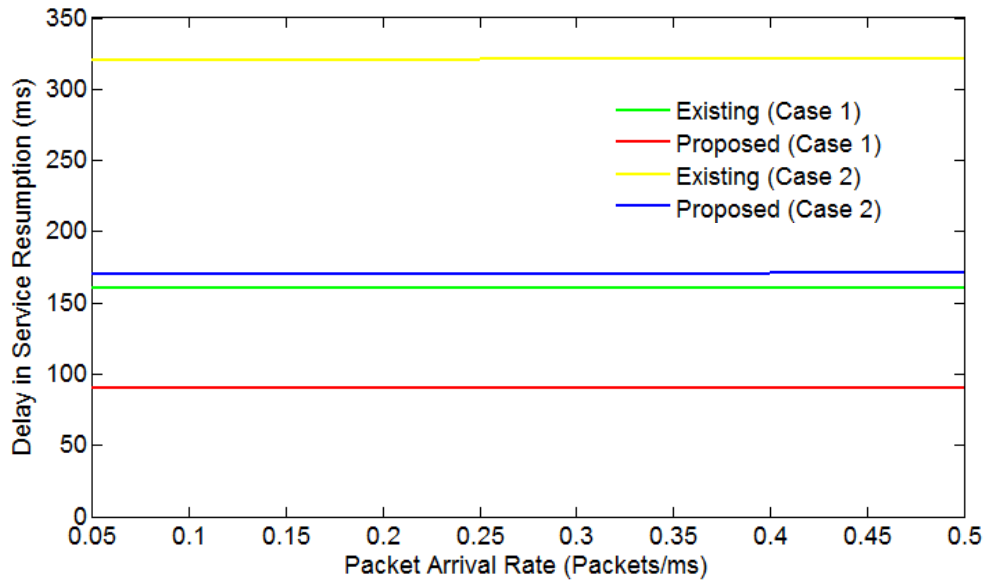
As shown in Fig. 6.5, compared to the benchmark, the proposed method has an increase in delay  $\Delta_{NRT} = 100 \text{ ms}$  for  $\lambda = 0.05 \text{ packets/ms}$ . This increased delay can be tolerable because  $\Delta_{NRT} \leq 107 \text{ ms}$ . Conversely, the delay in the existing method, even with  $N = 4$ , is almost 200 ms longer than the benchmark for  $\lambda = 0.05 \text{ packets/ms}$ . Thus, the existing method is not acceptable for small values of  $N$  as  $\Delta_{NRT} > 107 \text{ ms}$ . Consequently, the proposed method can be regarded as the best option.



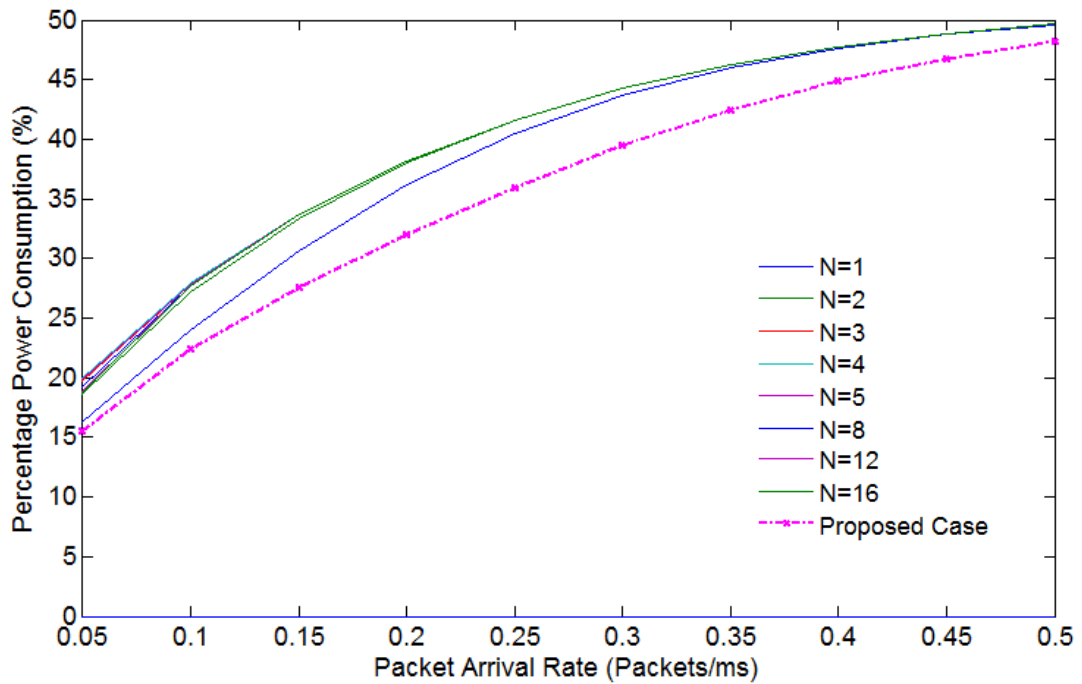
**Fig. 6.5** Overall packet delay vs. packet arrival rate (case 2)

Figure 6.6 shows that the mean delay in service resumption after a long inactivity for the proposed and existing methods for both case 1 and case 2. This delay is evidently much better in the proposed method.

In case 3, a small value of  $T_L$  is used. In this case, as Fig. 6.7 shows, the power saving becomes better in the proposed method compared to the existing method with any value of  $N$ .



**Fig. 6.6** Delay in service resumption vs. packet arrival rate (case 1 and case 2)



**Fig. 6.7** Percentage power consumption vs. packet arrival rate (case 3)

Figure 6.8 shows that all the cases here satisfy  $\Delta_{NRT} \leq 107 \text{ ms}$ .

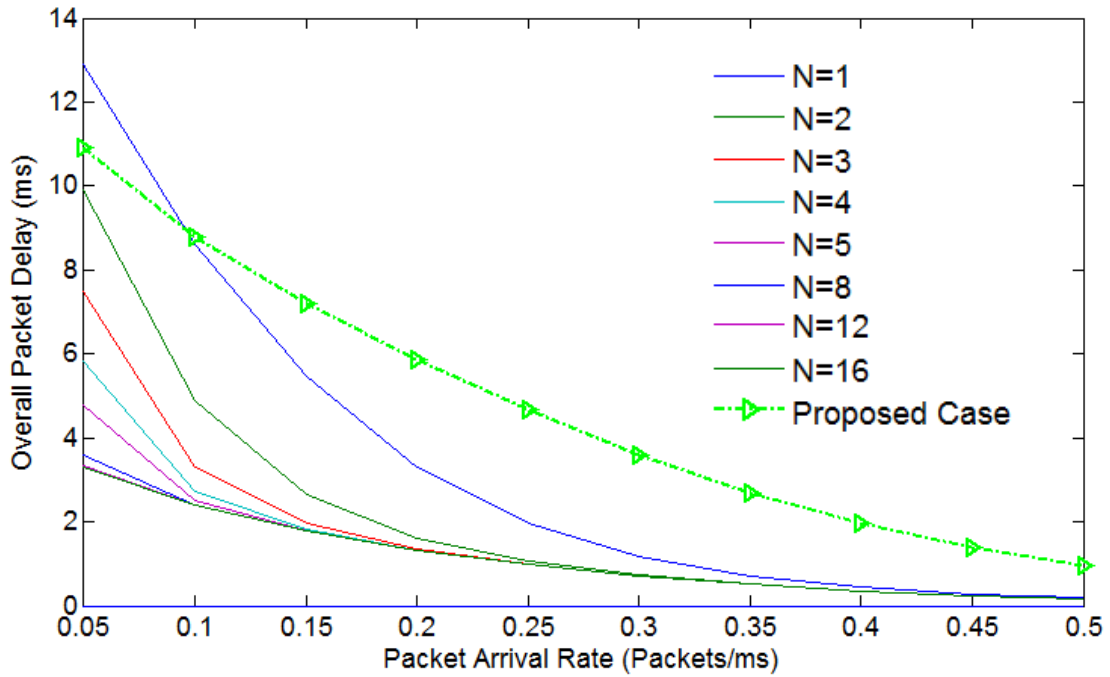


**Fig. 6.8** Overall packet delay vs. packet arrival rate (case 3)

In this chapter, the numerical examples demonstrate that a significantly better power saving is achieved in the proposed method with permissible increase in packet delay. The existing method may often attain an even better power saving setting very small values of  $N$  but its associated delay might exceed the tolerable limit then. The delay in service resumption after a long inactivity is always better in the proposed method.

## Chapter 7

---

# Conclusion

---

The purpose of our thesis has been to find a better power saving solution of the User Equipment (UE) for the LTE system as the higher data rates provided by the LTE system drains out the battery life of the UE more drastically.

For power saving in LTE system there is an existing Discontinuous Reception (DRX) mechanism which periodically turns off the receiver circuitry of the UE and thus reduce UE's power consumption. But this existing method suffers from the packet delay which actually refers to the time the data packet awaits to be allocated in the next On Duration of the DRX cycle.

So in our thesis, we present the tradeoff between power saving and delay for DRX operation in LTE. Since NRT applications are delay tolerant, to improve power saving, we propose a new DRX method to be applied when only NRT applications are running with no RT applications active.

The proposed method avoids the estimation of current traffic. It keeps varying the DRX cycle length in a simple fashion. We present analytical models to evaluate both the proposed and the existing methods. The numerical examples exhibit a conspicuous success in power saving in the proposed method.

We define a new factor for a more practical estimation of power saving. The proposed method also attains less mean delay in service resumption provided that there has been a long inactivity.

## 7.1 Future Works

The analytical model developed to perform this thesis analysis lends itself to be used to perform a quite big number of other studies that exploit any sort of combinations of the input parameters, added to the ones presented in the previous chapters.

The analytical system indeed can be fed with different NRT and RT applications if the delay budget is in the limit to exploit.

There is also a better scope to extend this model for the DRX mechanism in case of VoIP traffic.

---

## Bibliography

---

- [1] Mohammad T. Kawser, "LTE Air Interface Protocols", Artech House, ISBN: 978-1-60807-201-9, 2011.
- [2] Zhou, Lei, Haibo Xu, Hui Tian, Youjun Gao, Lei Du, and Lan Chen. "Performance analysis of power saving mechanism with adjustable DRX cycles in 3GPP LTE." In *Vehicular Technology Conference, (VTC 2008-Fall), IEEE 68th*, pp. 1-5, 2008.
- [3] Mihov, Yakim Y., Kiril M. Kassev, and Boris P. Tsankov. "Analysis and performance evaluation of the DRX mechanism for power saving in LTE." In *IEEE 26th Convention of Electrical and Electronics Engineers in Israel (IEEEI)*, pp. 000520-000524, 2010.
- [4] Fowler, Scott, Ranjeet S. Bhamber, and Abdelhamid Mellouk. "Analysis of adjustable and fixed drx mechanism for power saving in lte/lte-advanced." In *IEEE International Conference on Communications (ICC)*, pp. 1964-1969, 2012.
- [5] Wang, Hwang-Cheng, Chih-Cheng Tseng, Guan-Yun Chen, Fang-Chang Kuo, and Kuo-Chang Ting. "Power saving by LTE DRX mechanism using a mixture of short and long cycles." In *TENCON IEEE Region 10 Conference*, pp. 1-6, 2013.
- [6] Fowler, Scott, George Baravdish, and Di Yuan. "Numerical analysis of an industrial power saving mechanism in LTE." In *IEEE International Conference on Communications (ICC)*, pp. 1748-1753, 2014.
- [7] 3GPP TS 23.203, "Policy and charging control architecture." Rel. 12, v. 12.9.0, 2014.
- [8] F. X. Albizuri, M. Graña, B. Raducanu. "Statistical Transmission Delay Guarantee for Nonreal-Time Traffic Multiplexed with Real-Time Traffic." In *Computer Communications*, Vol. 26, Issue. 12, pp. 1365-1375, 2003.
- [9] Jha, Satish Chandra, Ali Taha Koc, and Rath Vannithamby. "Optimization of discontinuous reception (DRX) for mobile Internet applications over LTE." In *Vehicular Technology Conference (VTC Fall)*, pp. 1-5, IEEE, 2012.
- [10] Koc, Ali T., Satish Chandra Jha, Rath Vannithamby, and Murat Torlak. "Optimizing DRX configuration to improve battery power saving and latency of active mobile applications over LTE-A network." In *Wireless Communications and Networking Conference (WCNC)*, pp. 568-573. IEEE, 2013.



- [11] Liu, Yu, Minh Huynh, Anurag Mangla, and Dipak Ghosal. "Performance analysis of adjustable discontinuous reception (DRX) mechanism in LTE network." In *Wireless and Optical Communication Conference (WOCC)*, pp. 1-6. IEEE, 2014.
- [12] Rajesh, A., and R. Nakkeeran. "Performance analysis of enhanced DRX mechanism in LTE networks." In *International Conference on Computer Communication and Informatics (ICCCI)*, pp. 1-5. IEEE, 2014.
- [13] Karthik, R. M., and Arvind Chakrapani. "Practical algorithm for power efficient drx configuration in next generation mobiles." In *INFOCOM*, pp. 1106-1114. IEEE, 2013.
- [14] Koc, Ali T., Satish C. Jha, Rath Vannithamby, and Murat Torlak. "Device power saving and latency optimization in LTE-A networks through DRX configuration." In *IEEE Transactions on Wireless Communications*, Vol. 13, Issue no. 5, pp. 2614-2625. 2014.
- [15] Wang, Kangping, Xin Li, Hong Ji, and Xin Du. "Modeling and Optimizing the LTE Discontinuous Reception Mechanism under Self-Similar Traffic.", In *IEEE Transactions on Vehicular Technology*, Vol. PP, Issue no.99, pp.1-1, 2013.
- [16] Yu, Gwo-Jong. "A fuzzy adaptive DRX power saving mechanism for LTE-Advanced networks." In *The Fourth International Conference on Network of the Future (NOF)*, pp. 1-5, IEEE, 2013.
- [17] Zhang, Ziqi, Zhuyan Zhao, Hao Guan, Lei Du, and Zhenhui Tan. "Performance analysis of an adaptive DRX mechanism with flexible short/long cycle switching in LTE network." In *IEEE International Symposium on Microwave, Antenna, Propagation and EMC Technologies for Wireless Communications (MAPE)*, pp. 27-32, 2013.
- [18] 3GPP TS 36.331, "Radio Resource Control (RRC)", Rel. 12, v. 12.3.0, 2014.
- [19] Bontu, Chandra S., and Ed Illidge. "DRX mechanism for power saving in LTE." In *Communications Magazine, IEEE*, Vol. 47, Issue no. 6, pp. 48-55, 2009.
- [20] Jin, Sunggeun, and Daji Qiao. "Numerical analysis of the power saving in 3GPP LTE advanced wireless networks.", *IEEE Transactions on Vehicular Technology*, Vol. 61, Issue no. 4, pp. 1779-1785. IEEE, 2012.
- [21] S.-R. Yang and Y.-B. Lin, "Modeling UMTS discontinuous reception mechanism," *IEEE Trans. Wireless Commun.*, vol. 4, no. 1, pp. 312–319, Jan. 2005.
- [22] Gupta, Pragma Kirti, R. V. Rajakumar, C. Senthil Kumar, and Goutam Das. "Analytical evaluation of signalling cost on power saving mechanism in mobile networks." In *TENCON Spring Conference*, pp. 376-380, IEEE, 2013.
- [23] Varma, Syama, Krishna M. Sivalingam, Li-Ping Tung, and Ying-Dar Lin. "Analytical model for power savings in LTE networks using DRX mechanism." In *2015 Twenty First National Conference on Communications (NCC)*, pp. 1-6, IEEE, 2015.
- [24] Fowler, Scott. "Study on power saving based on radio frame in LTE wireless communication system using DRX." In *GLOBECOM Workshops (GC Workshops)*, pp. 1062-

1066. IEEE, 2011.

- [25] Wigard, Jeroen, Troels Kolding, Lars Dalsgaard, and Claudio Coletti. "On the user performance of LTE UE power savings schemes with discontinuous reception in LTE." In *IEEE International Conference on Communications Workshops, 2009. ICC Workshops 2009*, pp. 1-5. IEEE, 2009.
- [26] Zukerman, Moshe. "Introduction to Queuing Theory and Stochastic Teletraffic Models", <http://www.ee.cityu.edu.hk/Zukerman/classnote.pdf> (2000-2015).